

AD-A155 187

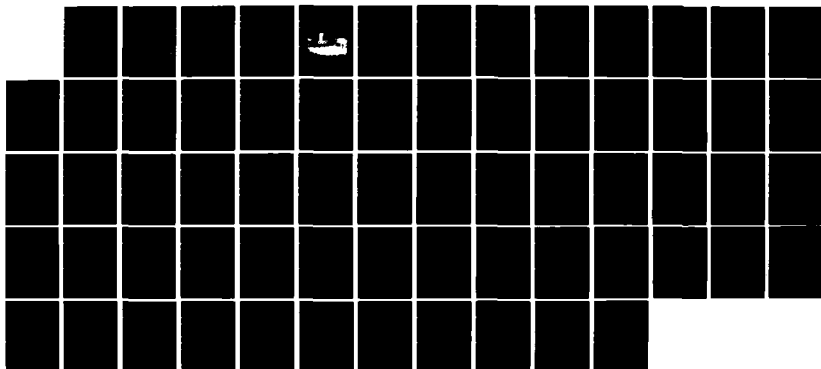
FLIGHTCONTROL SYSTEM FOR A COMPUTER CONTROLLED
AIRCRAFT WITH LIMITED SENSORS(U) AIR FORCE ACADEMY CO
T P WEBB 30 APR 85 USAFA-TN-85-4

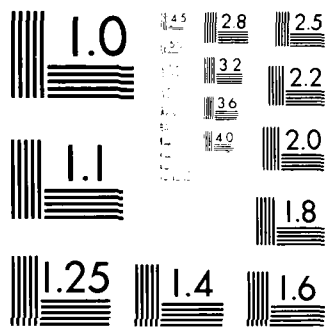
1/1.

UNCLASSIFIED

F/G 1/4

NL





MICROCOPY RESOLUTION TEST CHART
NATIONAL BUREAU OF STANDARDS-1963-A

2



Department of Aeronautics
Dean of the Faculty
United States Air Force Academy
Colorado 80840-5831

AD-A155 107

FLIGHT CONTROL SYSTEM FOR A COMPUTER
CONTROLLED AIRCRAFT WITH LIMITED SENSORS

TECHNICAL NOTE
USAFA-TN-85-4

Webb, T.P.

DTIC
ELECTE
JUN 19 1985
B

DTIC FILE COPY

30 APRIL 1985

APPROVED FOR PUBLIC RELEASE: DISTRIBUTION UNLIMITED

85 5 21 006

Any views expressed in this paper are those of the author. They should not be interpreted as reflecting the views of the USAF Academy or the official opinion of any governmental agency. Notes are not reviewed for content or quality by the USAF Academy but are published primarily as a service to the faculty to facilitate internal research communication.

This Technical Note has been cleared for open publication and/or public release by the appropriate Office of Information in accordance with AFR 190-17 and DODD 5230.9. There is no objection to unlimited distribution of this Technical Note to the public at large or by DDC to the National Technical Information Service.

This Technical Note is approved for publication.



Thomas E. McCann, Lt Colonel, USAF
Director of Research and Computer Based Education

✓	
PER CALL JC	
A-1	



FLIGHT CONTROL SYSTEM DESIGN FOR A COMPUTER CONTROLLED AIRCRAFT WITH LIMITED SENSORS

Thomas P. Webb*

Abstract

A complete flight control system for a small computer controlled aircraft was designed using only yaw rate, heading, lateral load factor, airspeed, altitude, and rate of climb feedback. This multi-input multi-output control problem was done using the classical root locus technique on a linearized system model. The performance of the flight control system was then checked using a 12 degree-of-freedom nonlinear simulation. The simulation results revealed surprisingly good performance, considering the limitation on sensors.

I. Introduction

The Department of Electrical Engineering at the United States Air Force Academy is attempting, through one of its senior design courses, to design, build, and fly a computer controlled aircraft. The Department of Aeronautics was asked to help design the flight control system to be implemented by the on-board digital computer. The project involved building and testing a wind tunnel model of the aircraft to determine its aerodynamic characteristics, performing mass tests on the actual aircraft to determine inertia characteristics, developing a 12 degree-of-freedom nonlinear aircraft simulation program, and designing the actual flight control system. This report describes only the last task.

II. Aircraft Description

The aircraft acquired by the Electrical Engineering Department is an off the shelf hobby radio controlled airplane called the "Big Stick" sold by Hobby Shack in kit form. This particular aircraft was chosen for its large size and docile handling qualities. The aircraft is

*Major, USAF, Assistant Prof., Dept. of Aeronautics, USAFA.

configured for normal radio controlled operation to allow for initial testing, manual backup/override for safety, and manual takeoffs and landings. The aircraft is propeller powered by a 2.5 brake horsepower (BHP) two-stroke-cycle gasoline Quadra 35 engine. The aircraft (see Fig. 1) has a wingspan of 8.73 feet. The estimated weight with full fuel and computer on board is 30 pounds. The tricycle landing gear configuration, as shown in the picture, was later modified to conventional (tail wheel) for structural reasons and to facilitate operation on grass.

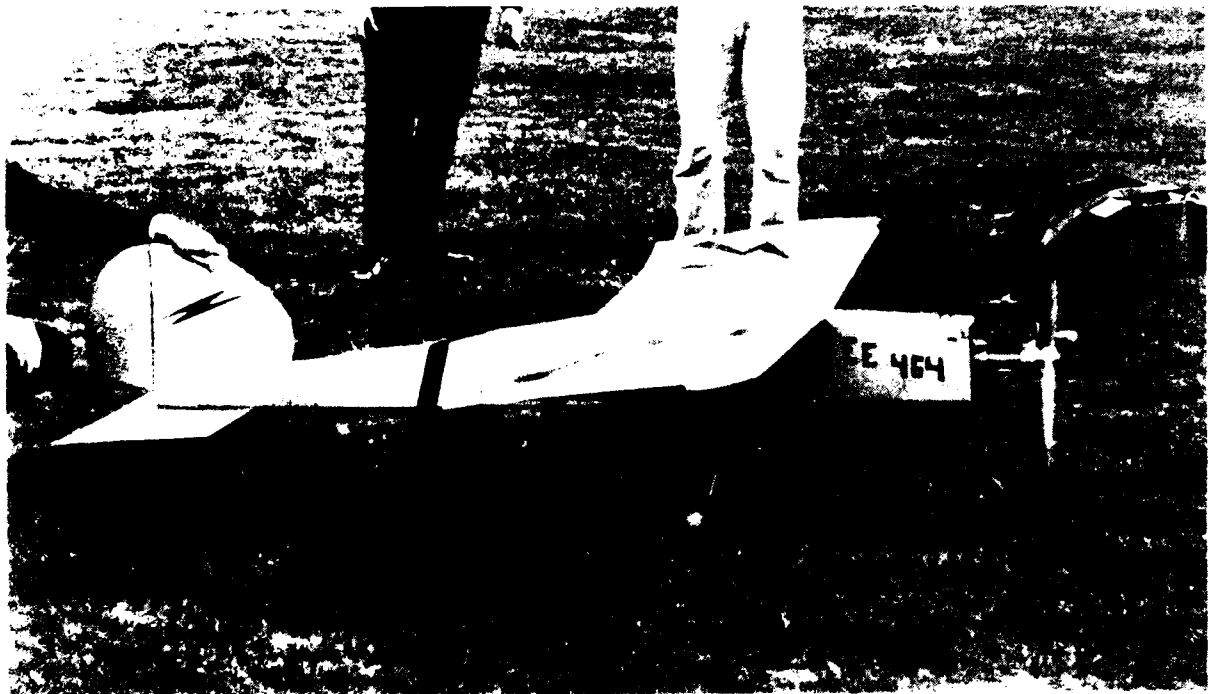


Figure 1. The Big Stick Airplane

The aircraft is controlled by conventional ailerons, rudder, elevator, and throttle. Drawings for the .122 scale wind tunnel model are contained in Appendix A.

III. The Control Problem

The purpose of the flight control system is to make the aircraft fly an arbitrarily specified (and not necessarily straight) path given continuous information on the current state of the aircraft through a limited number of sensors. The design of the flight control system was formulated as a multi-input multi-output feedback control problem. The actual parameters to be controlled were specified as altitude (h), airspeed (V), and heading (ψ).



Figure 2. The Control Problem

Referring to Figure 2, the control problem can be visualized as one of driving the values of h , V , and ψ to those of h_c , V_c , and ψ_c , respectively, where c denotes the commanded value.

The flight control system makes inputs to the aircraft by adjusting the settings or deflections of the elevator (δ_e), throttle (δ_T), ailerons (δ_a), and rudder (δ_r). These control settings depend on the sensor measurements, which contain information about the actual state of the aircraft, and the commanded values of altitude, airspeed, and heading. This process is depicted in Figure 3.

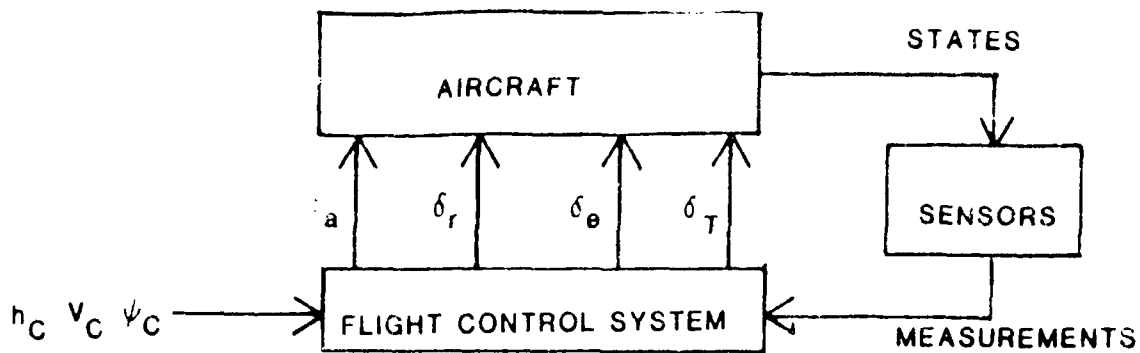


Figure 3. Control Process

The control system design problem, stated simply, was to find an algorithm to convert the commands and sensor measurements into the proper control settings to make the aircraft fly according to the commands.

Due to cost constraints, the sensors available for the project were limited to a yaw rate gyro, a lateral accelerometer, a heading indicator, an altimeter, and an airspeed meter. This is a very limited set of measurements considering the job required; therefore, it was feared that design of a satisfactory control system might prove impossible. For instance, note that there are no position gyros. This means that the control system is required to roll the aircraft in and out of turns with no feedback whatsoever as to the bank angle of the aircraft. Almost all three-axis autopilots in use today have position gyros for yaw, pitch, and roll angle measurements.

For design purposes, the measurements available to the flight control system were:

- n_y lateral load factor
- r yaw rate
- ψ heading

- h altitude
- V airspeed
- \dot{h} rate of climb (to be derived by numerically differentiating h)

IV. Design Procedure

"Classical" control theory methods (LaPlace tranforms and root loci) were used in the design of this control system as opposed to "modern" optimal control techniques (although the state-space matrix representation was borrowed from modern theory).

Two important simplifications were made and carried throughout the entire design procedure. The first was that the control system was continuous instead of discrete. (Recall that the control system is to be implemented by a digital computer.) This assumption is not too unreasonable provided the cycle time of the computer is quite a bit faster than the aircraft response. The second simplification was that of perfect sensors. This means that the measurements of the aircraft's state provided to the control system are true and uncorrupted by noise. This simplification may or may not be valid, depending on the quality of the sensors. As is the case in many feedback control design problems, the sensors were of minor concern during the design process, but their performance will make or break the flight control system when it is implemented in the actual aircraft.

The design procedure consisted of four major steps:

1. Determining the control system structure
2. Formulating the complete system linear model
3. Selecting the control system gains
4. Checking the control system performance in a nonlinear simulation.

A. Control System Structure

The control system structure or framework was arrived at by paralleling the way a pilot flies an aircraft in instrument conditions without attitude information. (This type of flying is referred to as "needle, ball, and airspeed" flying and is normally only done as an emergency procedure following an attitude indicator failure.) The structure is shown in the block diagram in Figure 4.

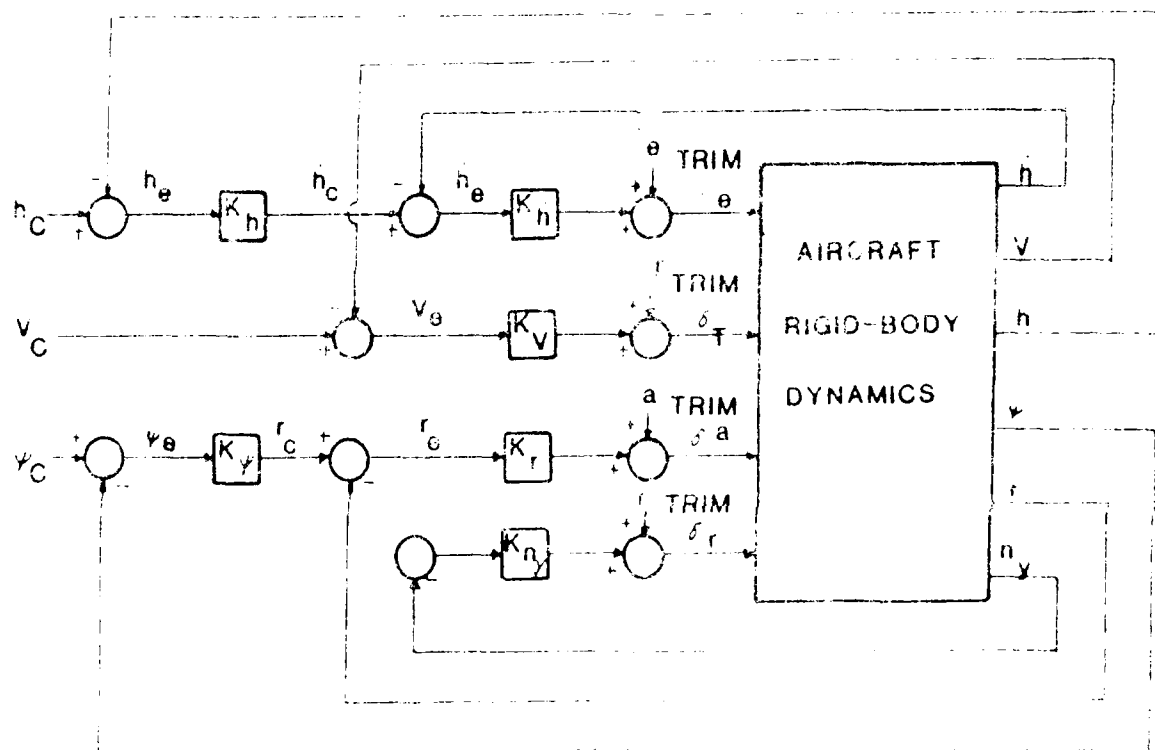


Figure 4. Flight Control System Structure (Basic)

In the block diagram (Figure 4), the square root of the error signal is used to produce the input signal to the controller, K . An error is defined as zero. The circles represent summing junctions and output. The subscript c denotes a command value, e denotes error. The subscript r denotes a reference value. The subscript y denotes a measured value. The subscript h denotes the altitude, v denotes the velocity, r denotes the heading, δ denotes the control signal, δ_e denotes the error signal, δ_v denotes the velocity error signal, δ_r denotes the heading error signal, δ_a denotes the acceleration error signal, δ_n denotes the normal acceleration error signal, δ_y denotes the yaw error signal, δ_z denotes the roll error signal, δ_x denotes the pitch error signal, δ_t denotes the time error signal, δ_s denotes the speed error signal, δ_d denotes the distance error signal, δ_a denotes the acceleration error signal, δ_n denotes the normal acceleration error signal, δ_y denotes the yaw error signal, δ_z denotes the roll error signal, δ_x denotes the pitch error signal, δ_t denotes the time error signal, δ_s denotes the speed error signal, δ_d denotes the distance error signal.

1. The first part of the report is a summary of the work done during the year.

2. The second part is a detailed account of the work done during the year.

3. The third part is a summary of the work done during the year.

4. The fourth part is a summary of the work done during the year.

5. The fifth part is a summary of the work done during the year.

6. The sixth part is a summary of the work done during the year.

7. The seventh part is a summary of the work done during the year.

8. The eighth part is a summary of the work done during the year.

9. The ninth part is a summary of the work done during the year.

10. The tenth part is a summary of the work done during the year.

11. The eleventh part is a summary of the work done during the year.

12. The twelfth part is a summary of the work done during the year.

13. The thirteenth part is a summary of the work done during the year.

14. The fourteenth part is a summary of the work done during the year.

(15)

15. The fifteenth part is a summary of the work done during the year.

16. The sixteenth part is a summary of the work done during the year.

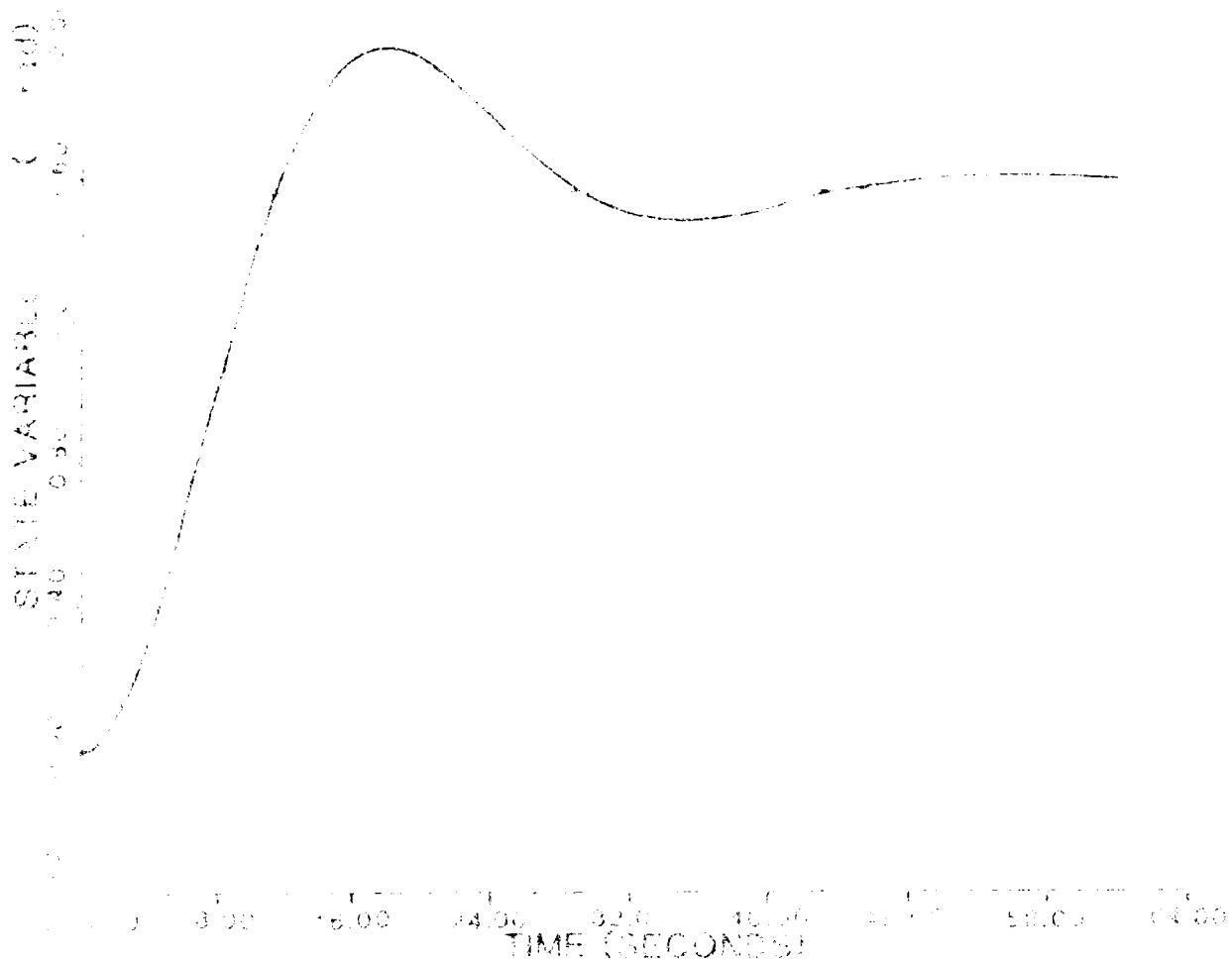
17. The seventeenth part is a summary of the work done during the year.



1. The first part of the curve is a straight line from the origin to the point (1, 1). This represents the initial phase of the process, where the rate of change is constant.

2. The second part of the curve is a curve that starts at (1, 1) and rises steeply, then levels off towards the right. This represents the phase of rapid growth, where the rate of change is increasing.

3. The third part of the curve is a curve that starts at (10, 8.5) and levels off towards the right. This represents the phase of slow growth, where the rate of change is decreasing.



FLIGHT HISTORY

0.00 0.00 0.00 0.00 0.00 0.00 0.00 0.00 0.00

the wing stall. The results are shown in Figures 17, 18, and 19. Figure 17 shows the heading again over the 15 second period. The heading value from Figure 18 we can see that the aircraft levels off at a value slightly below 7000 feet. Figure 19 shows that the velocity goes through some gyrations. It stabilizes at about 75 ft/s in the descent and then reduces to about 62 ft/s when the aircraft pulls out of the turn. Figure 20 is a plot of the throttle activity during this maneuver. It shows the throttle at idle from the 5 to 13 second point. The throttle then goes up to about 1.15 and stays there for a moment and then comes up to about 1.8 BHP after the aircraft levels out.

B. Simulation

Simulations with the selected gains were run using the nonlinear simulation program of Appendix D. Limitations on control deflections and on some of the gains were added for reasons discussed in the last section. Four flight maneuvers were simulated. The initial conditions for each maneuver were the steady-state reference condition (straight and level with $\alpha=0$, $V=73.33$ ft/s, and $h=7500$ ft). The four maneuvers were:

- (1) level turn
- (2) straight climb
- (3) level, straight acceleration
- (4) combination turn, descent, and deceleration

1. Nonlinear Limits

The following control limits were used in the simulation based on estimated aircraft limits:

control	min.	max.
δ_a	-15 deg	15 deg
δ_T	0 BHP	2 BHP
δ_r	-15 deg	15 deg
$\delta_{\dot{h}}$	-15 deg	15 deg

Limits on commanded rate of climb (\dot{h}_c) were selected as ± 11.5 ft/s.

This corresponds to climb and descent angle of nine degrees. The

climb would require about 2 BHP at steady state. The commanded turn

rate limit was limited as ± 0.1 rad/s. This equates to a bank angle of about 1.5 degrees and a turn radius of about 6,000 feet.

a. level turn simulation

A maneuver to a heading of 150 deg (1.92 rad) was required. The aircraft response is plotted in Figure 11.13. The

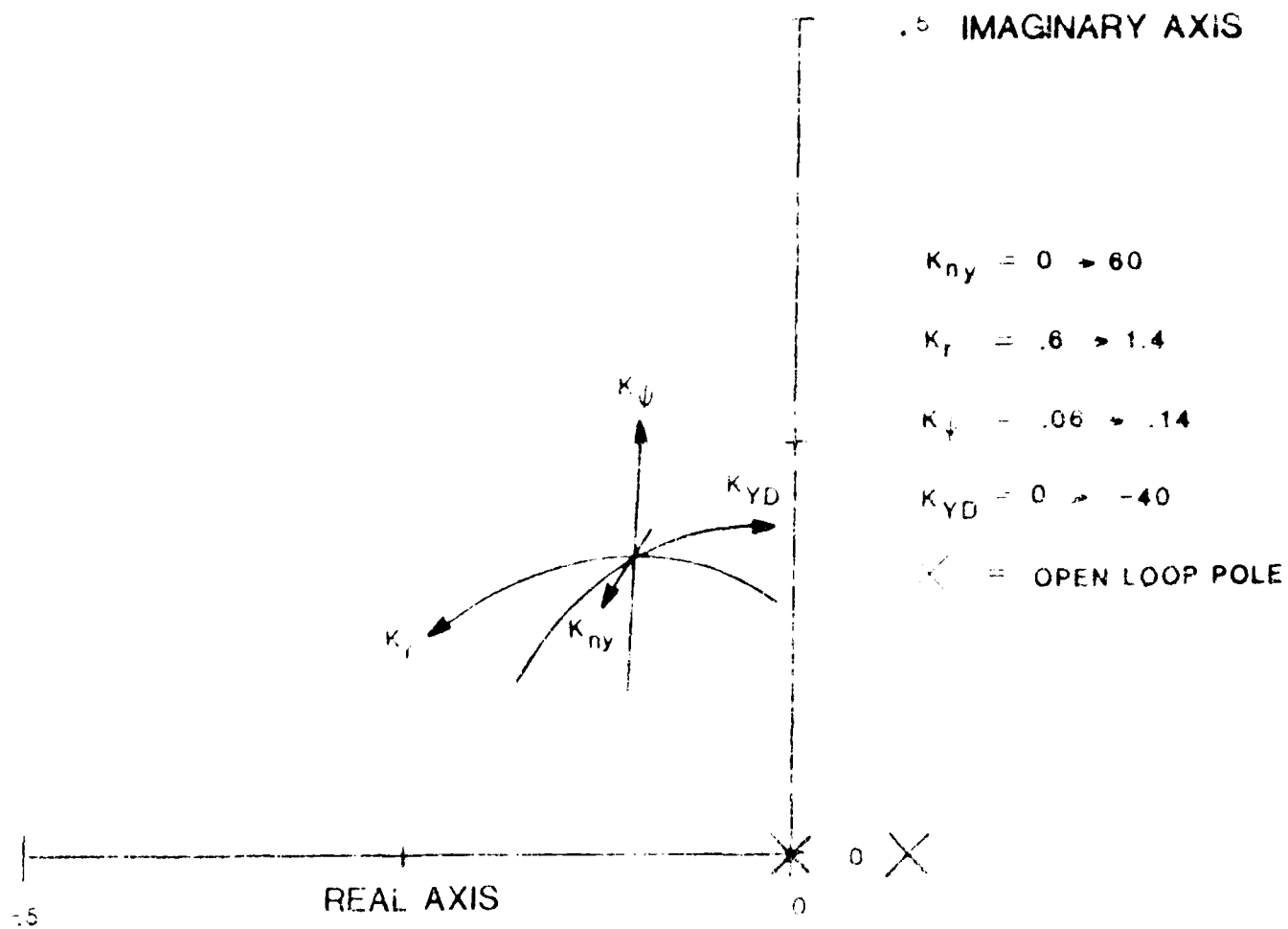


Figure 9. Lateral-Directional Root Loci (Blow-up)

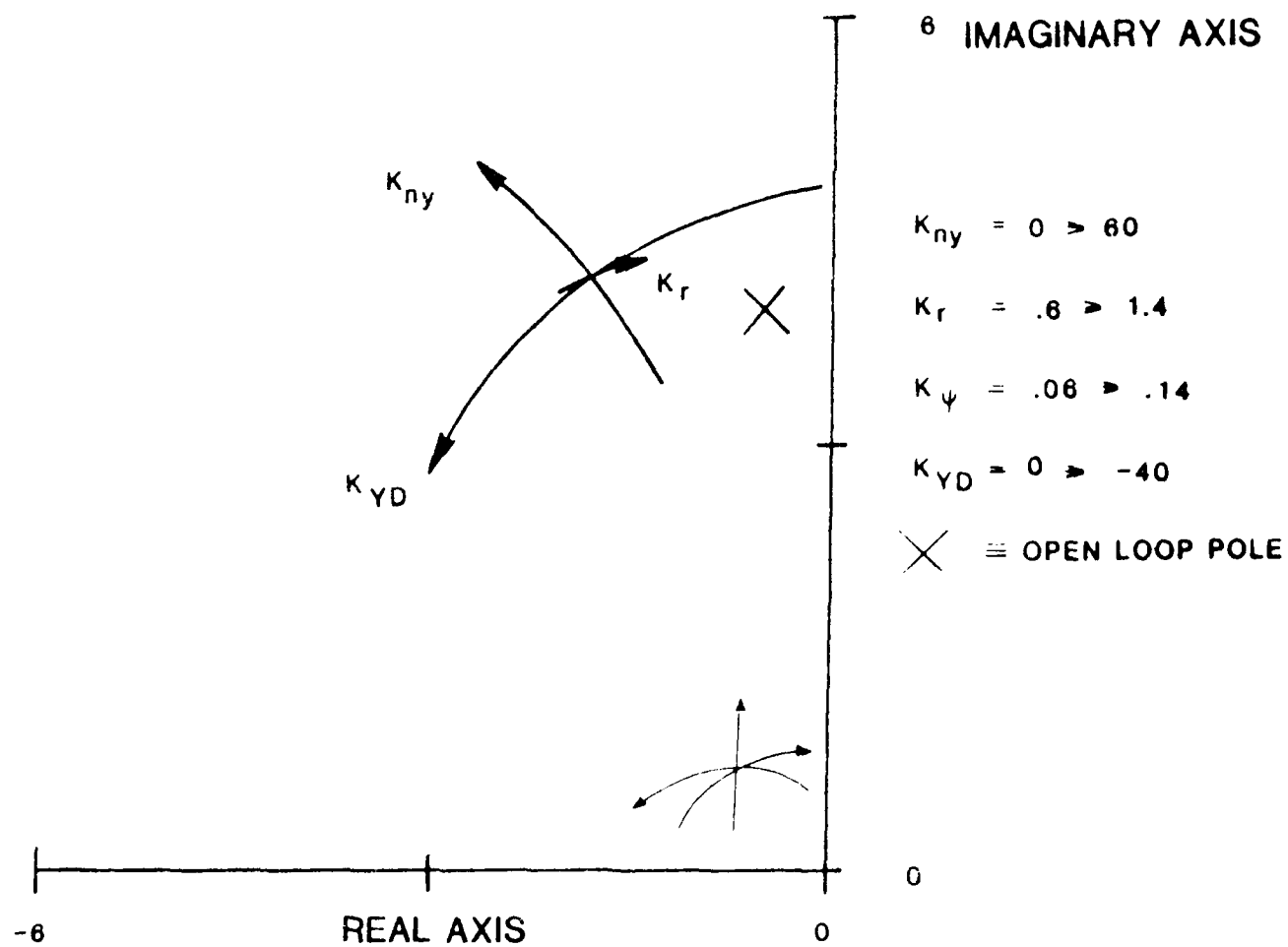


Figure 8. Lateral-Directional Root Loci

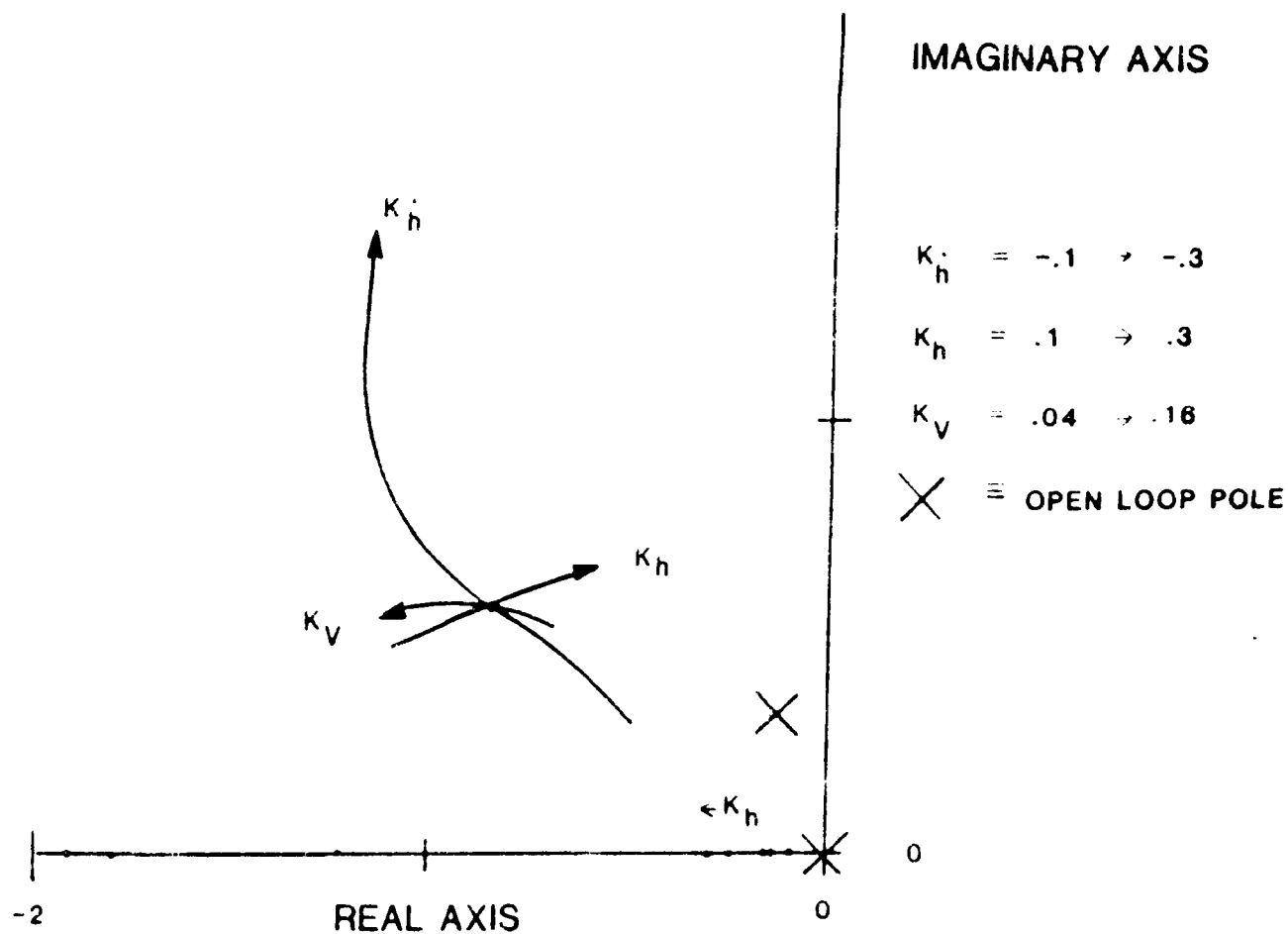


Figure 7. Longitudinal Root Loci

2. Lateral-directional case

The four lateral-directional gains selected were: $K_{ny} = 30$ deg/rad/sec, $K_r = 1$ rad/s/rad, and $K_{YD} = 20$ deg/rad/s. Figures 8 and 9 are the lateral-directional root loci plots. Figure 9 is a blow-up of the area around the origin in Figure 8. Again, a computer printout of the poles for each set of gains plotted is

tabulated in Appendix L.

The simulation results for the selected gains are presented in the next section.

V. Results

A. Root Loci

In multi-loop feedback systems, such as the one being dealt with in this report, the gains affect the system poles in an interrelated and complex fashion. A "shotgun" (trial and error) approach was used to initially find a neighborhood of gains that appeared to give reasonable poles. The gains were then varied in a more systematic fashion to refine the gain selection. Gains were selected on the basis of the speed and stability of the resulting poles. This was done separately for the longitudinal and lateral-directional cases.

1. Longitudinal case

The three longitudinal gains selected were:

$K_{\theta} = -.2 \text{ deg/ft/s}$, $K_h = .2 \text{ ft/s/ft}$, and $K_V = .1 \text{ BHP/ft/s}$. Figure 7 shows a segment of the longitudinal root loci plot that indicates how the poles are affected by the gains around the selected values. Only the upper left quadrant of the complex plane is shown since any values in the right half plane are unstable and unacceptable and since the bottom half plane is a mirror image of the top. The actual values of the poles plotted are contained in the computer printout in Appendix E.

gains.

The root loci were constructed by varying the gains and solving for the poles after each change. This process had to be computerized. Separate programs were written on an Apple microcomputer for the longitudinal and lateral-directional cases. The results are discussed in the next section.

D. Nonlinear Simulation

A 12 degree of freedom nonlinear Big Stick simulation program was written for the Burroughs 6900 computer at the Air Force Academy by Cadet First Class Daniel A. Draeger. A hard copy is included in Appendix D. This simulation provides a much more accurate mathematical model of the aircraft than the linearized equations which were used to determine the control gains. Basically, the program numerically integrates the nonlinear aircraft equations of motion from Reference 1, modified to include the control system, and plots out any of the state variables versus time. The nonlinear equations do not decouple into longitudinal and lateral-directional sets.

The simulation was run to see how the control gains, selected under the linear assumption, would actually perform in the real, nonlinear world. The effects of such elements as control deflection limits and changes in air density could be observed. The simulation was also used to check the limiting values for r_c and \dot{h}_c . These are cutoff values which had to be incorporated into K_h and $K_{\dot{h}}$ to prevent the aircraft from stalling itself out or entering a steep dive in the case of a big change in h_c or rolling inverted when r_c changed. A side benefit of the simulation is that it provides a check on the previous calculations. Performance should be close to the linear prediction around the steady-state condition.

pole indicates the stability of its associated mode (- for stable, + for unstable, 0 for neutral) and the imaginary part indicates the oscillation frequency (aperiodic if real). Complex poles occur in conjugate pairs. The magnitude of the pole (distance from origin) indicates the speed of the associated mode. For example, in Figure 6, poles 1, 2, and 5 are aperiodic. Poles 1 and 5 are stable while 2 is unstable. The mode associated with pole 5 will die out faster than the one associated with pole 1. The complex conjugate pairs 3 and 4 represent oscillatory modes. Mode 3 is stable and 4 is unstable.

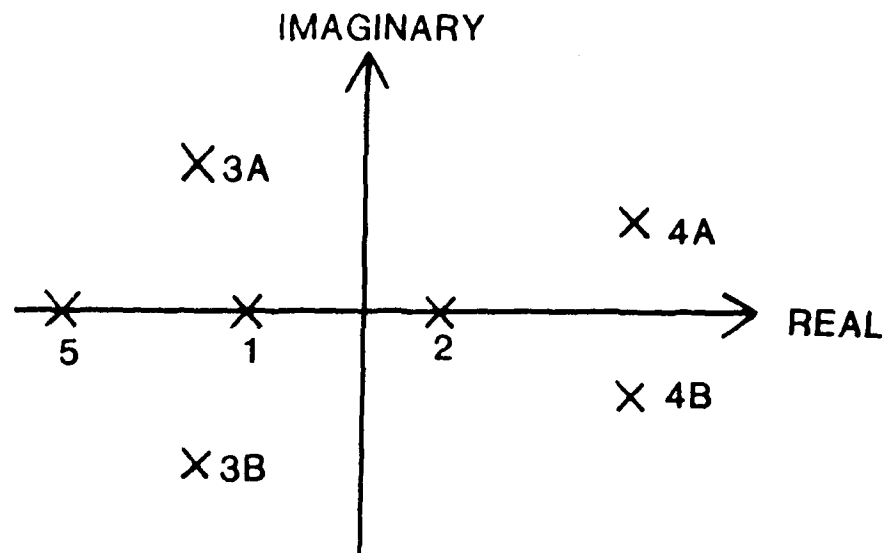


Figure 6. Poles on the Complex Plane

It can be shown (Ref. 4) that the characteristic equation of a system described by Equation 3 is $\det(\lambda[I] - [A]) = 0$ where λ is an arbitrary scalar number and $[I]$ is an identity matrix. The solutions of the equation for λ are the poles. We are interested in the poles of the closed-loop system, Equation 10. These can be determined by solving $\det(\lambda[I] - [A-BF]) = 0$. The F matrix, of course, depends on the

For the lateral-directional model:

$$[F] = \begin{bmatrix} 0 & 0 & K_r & 0 & K_\psi K_r \\ 1.22K_{ny} & .000634K_{ny} & K_{YD} - .0285K_{ny} & 0 & 0 \\ 1 - .00624K_{ny} & 1 - .00624K_{ny} & 1 - .00624K_{ny} & 0 & 0 \end{bmatrix} \quad (7)$$

$$[B'] = \begin{bmatrix} K_\psi K_r & 0 \\ 0 & 0 \end{bmatrix} \quad (8)$$

By substituting (4) into (3), we obtain

$$\dot{\bar{x}} = [A] \bar{x} + [B] \{-[F] \bar{x} + [B'] \bar{u}_c\}. \quad (9)$$

Combining terms gives

$$\dot{\bar{x}} = [A - BF] \bar{x} + [BB'] \bar{u}_c \quad (10)$$

The complete linearized system model (or closed-loop system), then, consists of two independent equations of the form of Equation 10 -- one for longitudinal motion and one for lateral-directional motion. The vectors and constant matrices have been defined for each case.

C. Determination of Control System Gains

The core of the feedback control problem is the selection of the control gains. In this project, that means finding values of K_h , K_ψ , K_V , K_r , K_{ny} , and K_{YD} that give satisfactory response to aircraft heading, altitude, and airspeed commands in the presence of disturbances such as wind gusts.

The response of any linear dynamic system is characterized by the roots of its characteristic equation (also called system poles or eigenvalues). Root loci were used in this project to select the gains. A root locus is a complex plane plot showing how a pole varies as a gain is changed. By way of review, the sign of the real part of the

algebraic combinations of the states. Equation 1 shows that this is true for the measurement \dot{h} . This is also true for n_y^1 . V is closely approximated by u . It is possible, then, in both the longitudinal and lateral-directional cases to express the controls as:

$$\bar{u} = - [F] \bar{x} + [B'] \bar{u}_c \quad (4)$$

where $[F]$ is called the feedback matrix and $[B']$ is called the input matrix. The vector \bar{u}_c is the command which is defined as $[h_c, V_c]^T$ for the longitudinal case and $[\psi_c, 0]^T$ for the lateral-directional case.

From Figure 5 and Equation 1 and 2 the feedback and input matrices were determined to be as follows:

For the longitudinal model:

$$[F] = \begin{bmatrix} 0 & 73.33K_h^* & 0 & -73.33K_h^* & K_h K_h^* \\ 0 & 0 & K_v & 0 & 0 \end{bmatrix} \quad (5)$$

$$[B'] = \begin{bmatrix} K_h K_h^* & 0 \\ 0 & K_v \end{bmatrix} \quad (6)$$

¹ n_y is lateral load factor which is equal and opposite to nongravitational lateral acceleration, normalized to the acceleration of gravity, g . It can be shown from Reference 1 and Appendix C that for the linearized approximation, $n_y = 1.222\beta + .000634p - .0285 r - .00624\delta_r$, which is a linear, algebraic combination of the states. (δ_r is a combination of the states only, since there are no commands that feed into the rudder.)

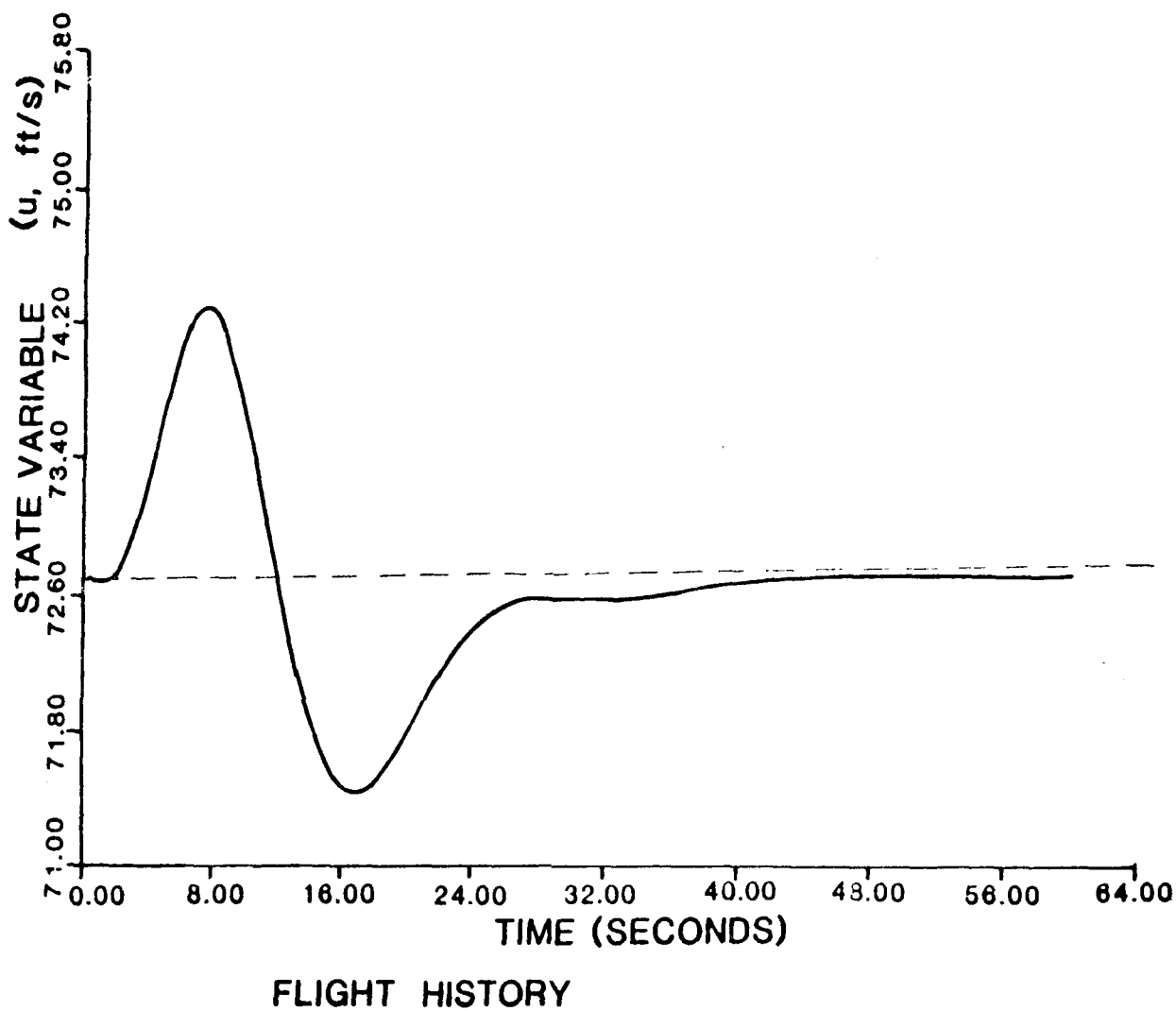
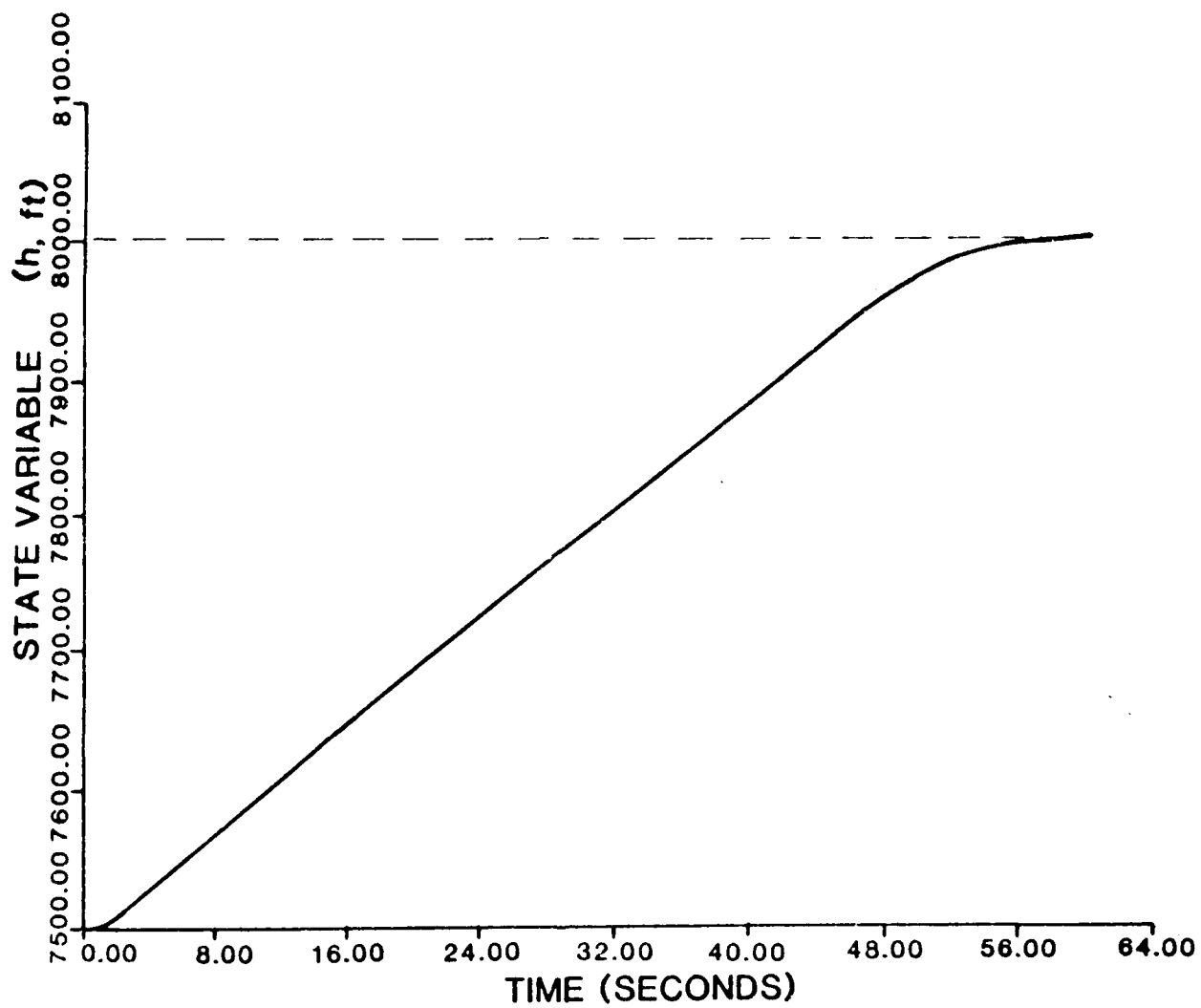
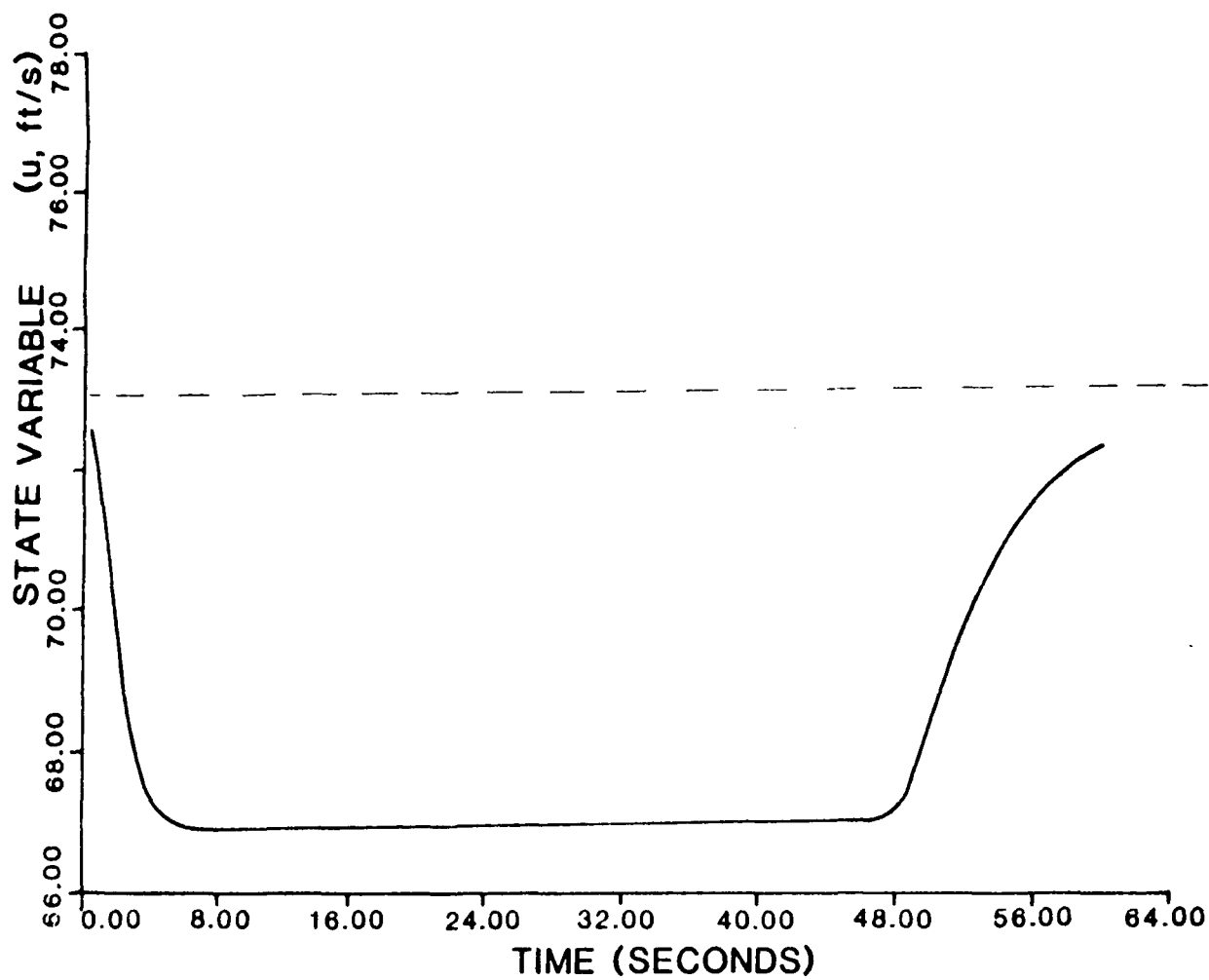


Figure 13. Level Turn Simulation - u



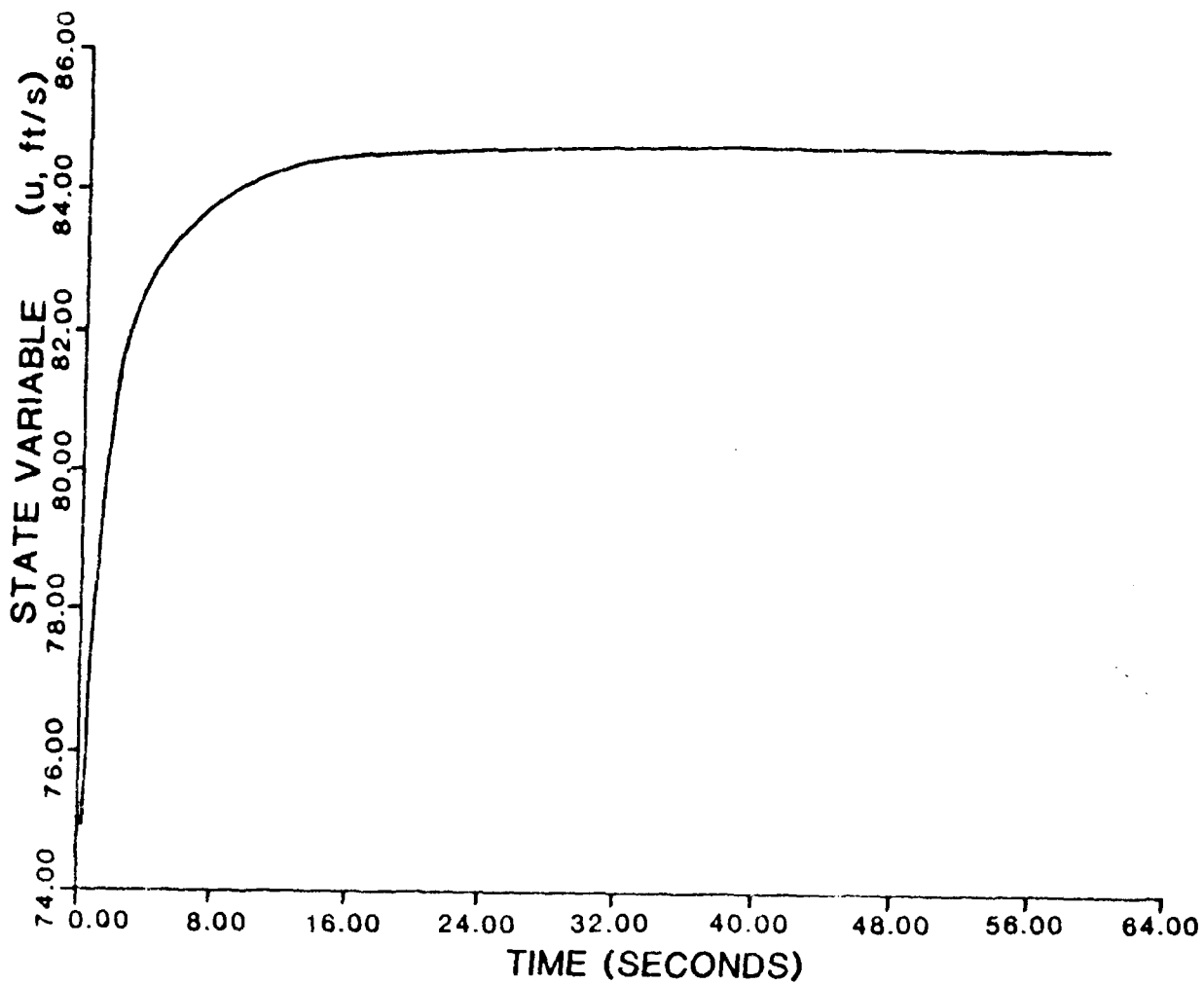
FLIGHT HISTORY

Figure 14. Straight Climb - h



FLIGHT HISTORY

Figure 15. Straight Climb Simulation - u



FLIGHT HISTORY

Figure 16. Level Acceleration Simulation - u

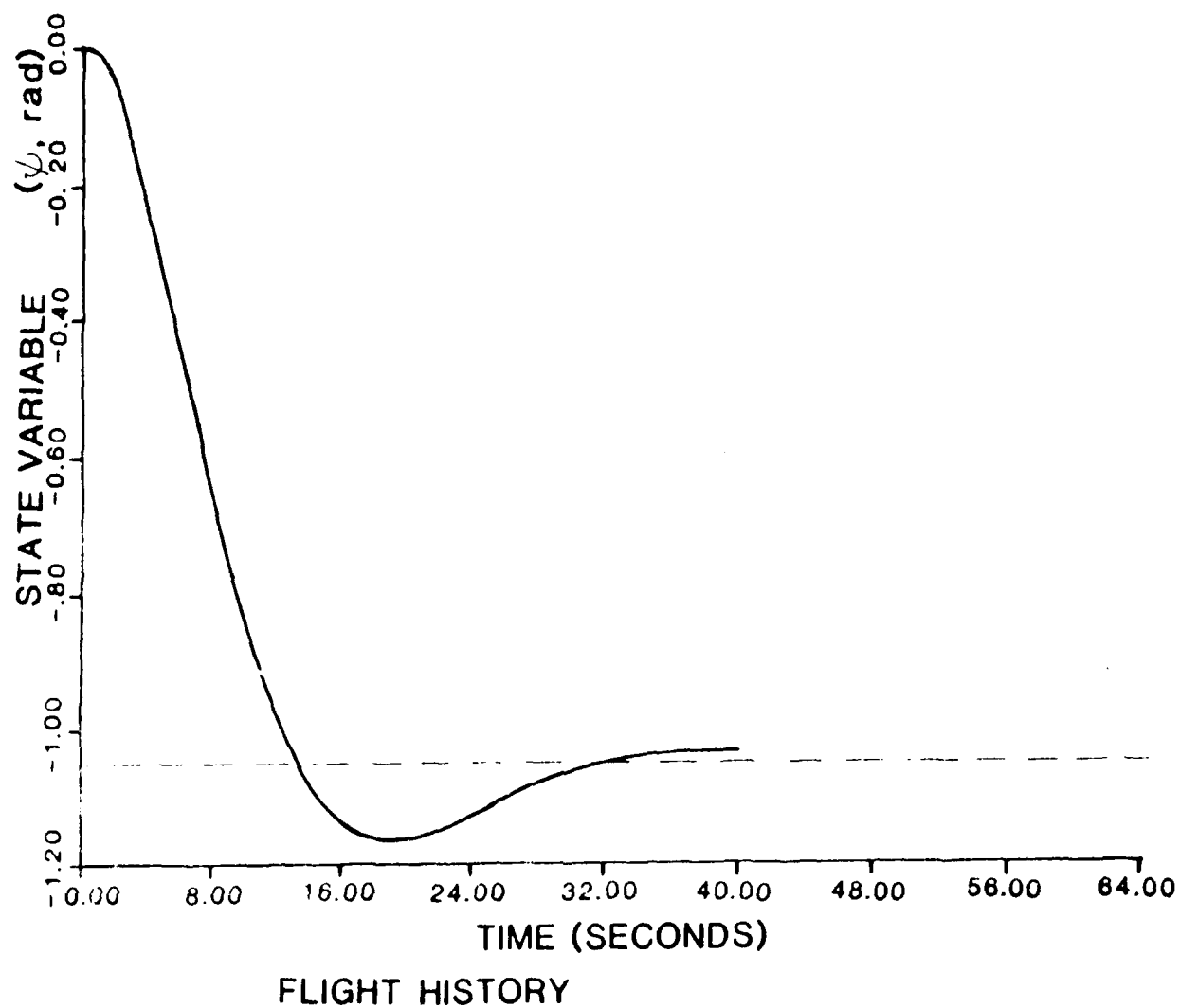
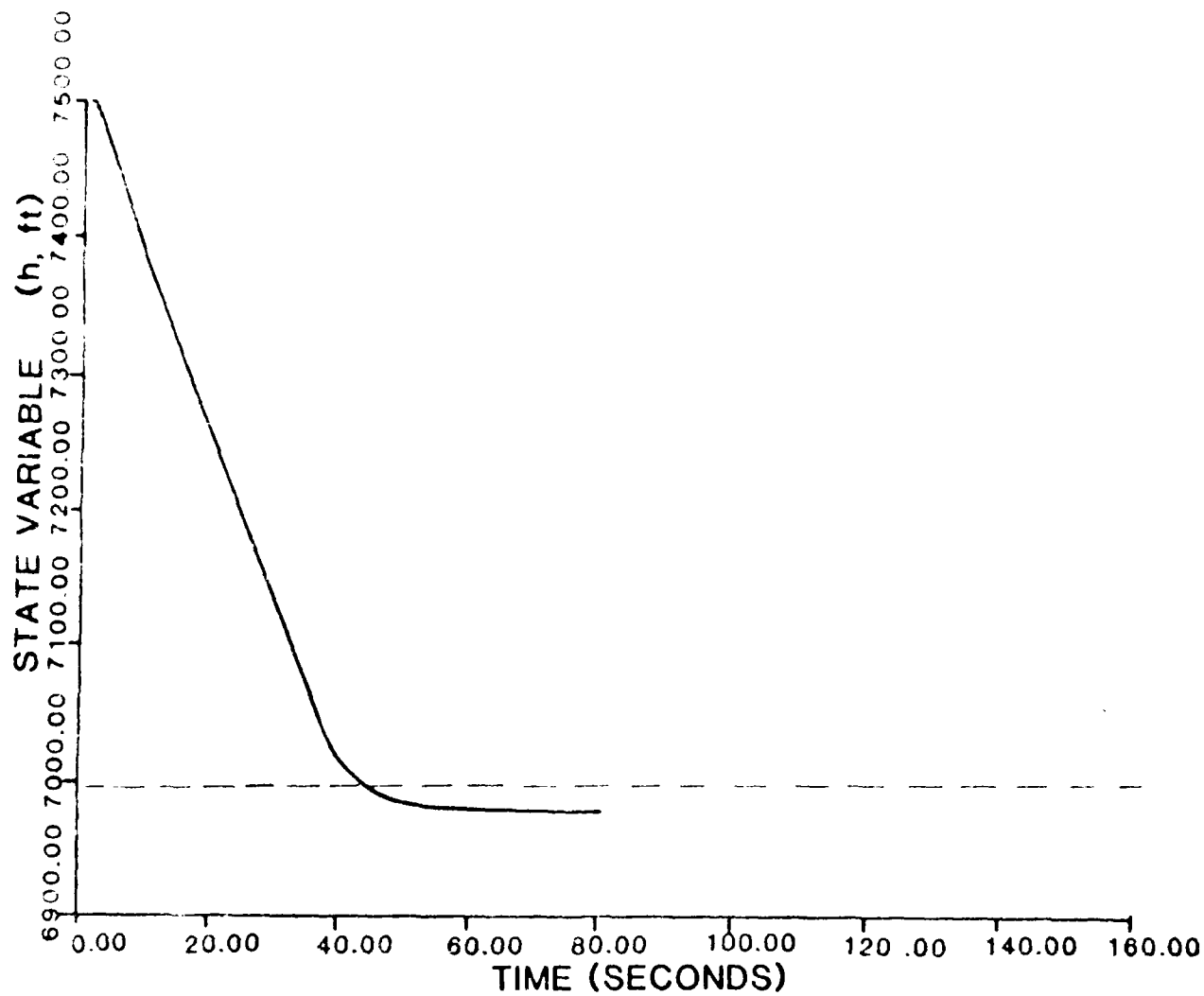
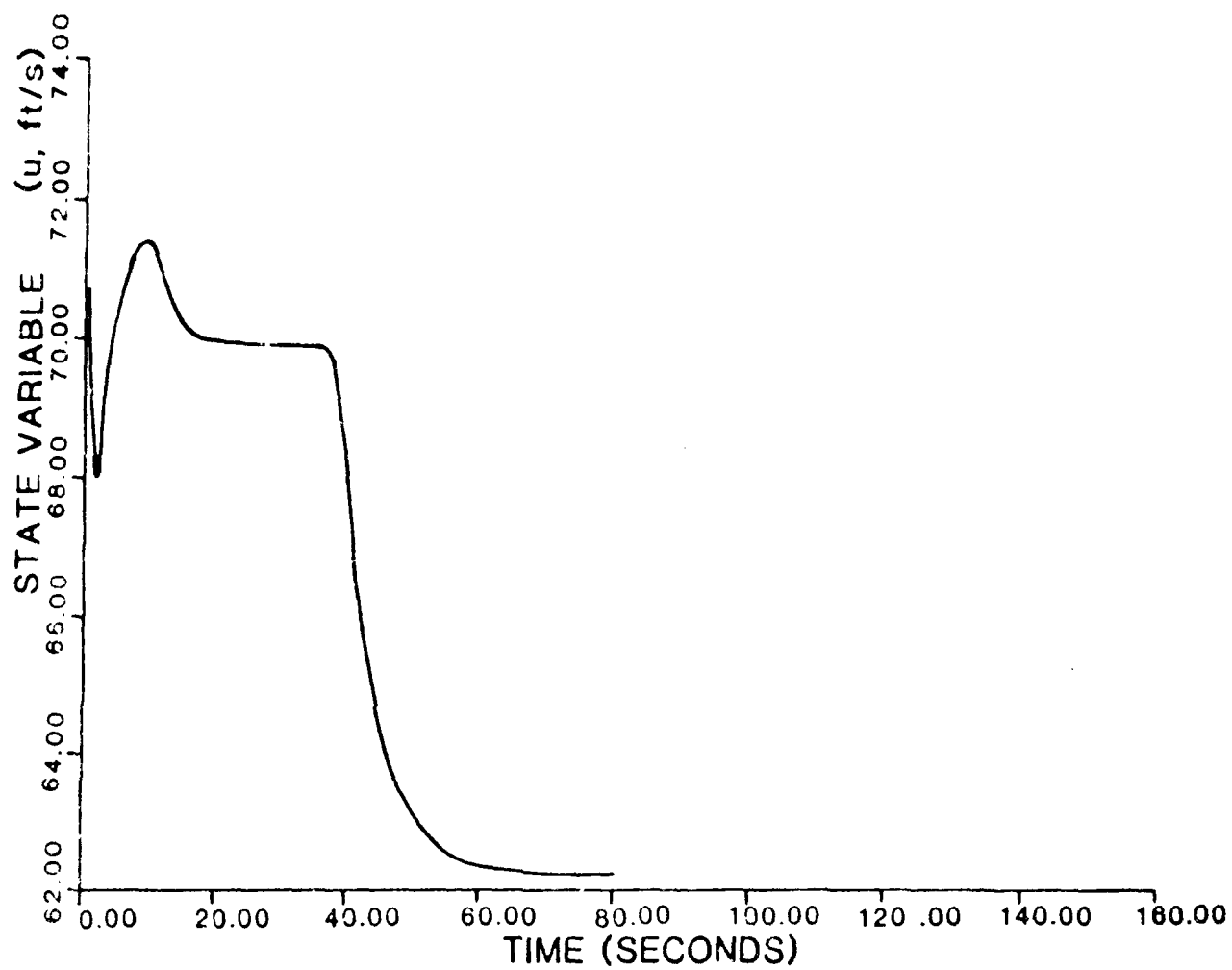


Figure 17. Multi-command Simulation - ψ



FLIGHT HISTORY

Figure 18. Multi-command Simulation - h



FLIGHT HISTORY

Figure 19. Multi-command Simulation - u

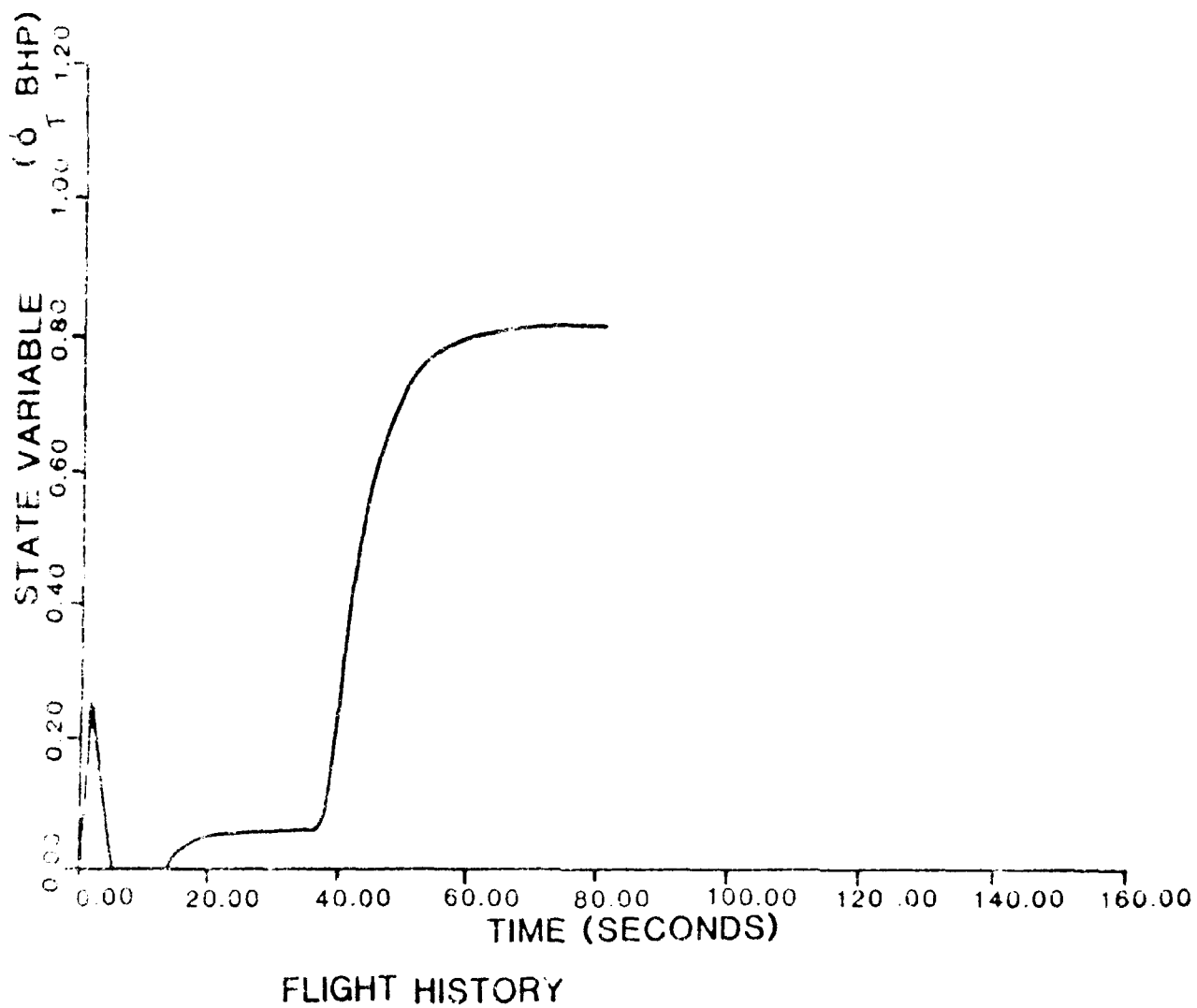


Figure 20. Multi-command Simulation - δ_1

VI. Recommendations

Based on the previous analysis, the following recommendations are made for the Big Stick flight control system:

1. That the control structure of Figure 5 be used.
2. That the following control gains be used:

$$K_{\dot{h}} = 1.2 \text{ (ft/s)/ft}$$

$$K_{\dot{h}} = -1.2 \text{ deg/(ft/s)}$$

$$K_V = 1.1 \text{ BHP/(ft/s)}$$

$$K_{\dot{\phi}} = 1 \text{ (rad/s)/rad}$$

$$K_{\dot{\phi}} = 1 \text{ deg/(rad/s)}$$

$$K_{\dot{\psi}} = 30 \text{ deg/g}$$

$$K_{YD} = -20 \text{ deg/(rad/s)}$$

3. That \dot{h}_C be limited to ± 11.5 ft/s and $\dot{\phi}_C$ be limited to ± 12 rad/s.
4. That a washout filter be included in the yaw damper feedback loop to pass the dutch roll frequency (4 rad/s) and attenuate the steady-state commanded yaw rate.
5. That the trim control settings be determined from flight test at the steady-state flight condition of straight and level at 73.33 ft/s and 7500 feet.

In implementing the flight control system, the same sign conventions must, of course, be used as are used in the aircraft equations of motion. These are (from Appendices C and D and Reference 1):

1. Positive for trailing edge down

2. Positive for trailing edge left

3. Positive for right up and left down $\omega = (\omega_1 + \omega_2)/2$

4. Positive to right

1. Introduction

2. Background

3. Literature

1. J. H. Davenport, "The Dynamics of Shipboard Control Systems," *Journal of Ship Research*, Vol. 1, No. 1, 1957, pp. 1-10.

2. J. H. Davenport, "The Dynamics of Shipboard Control Systems," *Journal of Ship Research*, Vol. 1, No. 1, 1957, pp. 1-10.

3. J. H. Davenport, "The Dynamics of Shipboard Control Systems," *Journal of Ship Research*, Vol. 1, No. 1, 1957, pp. 1-10.

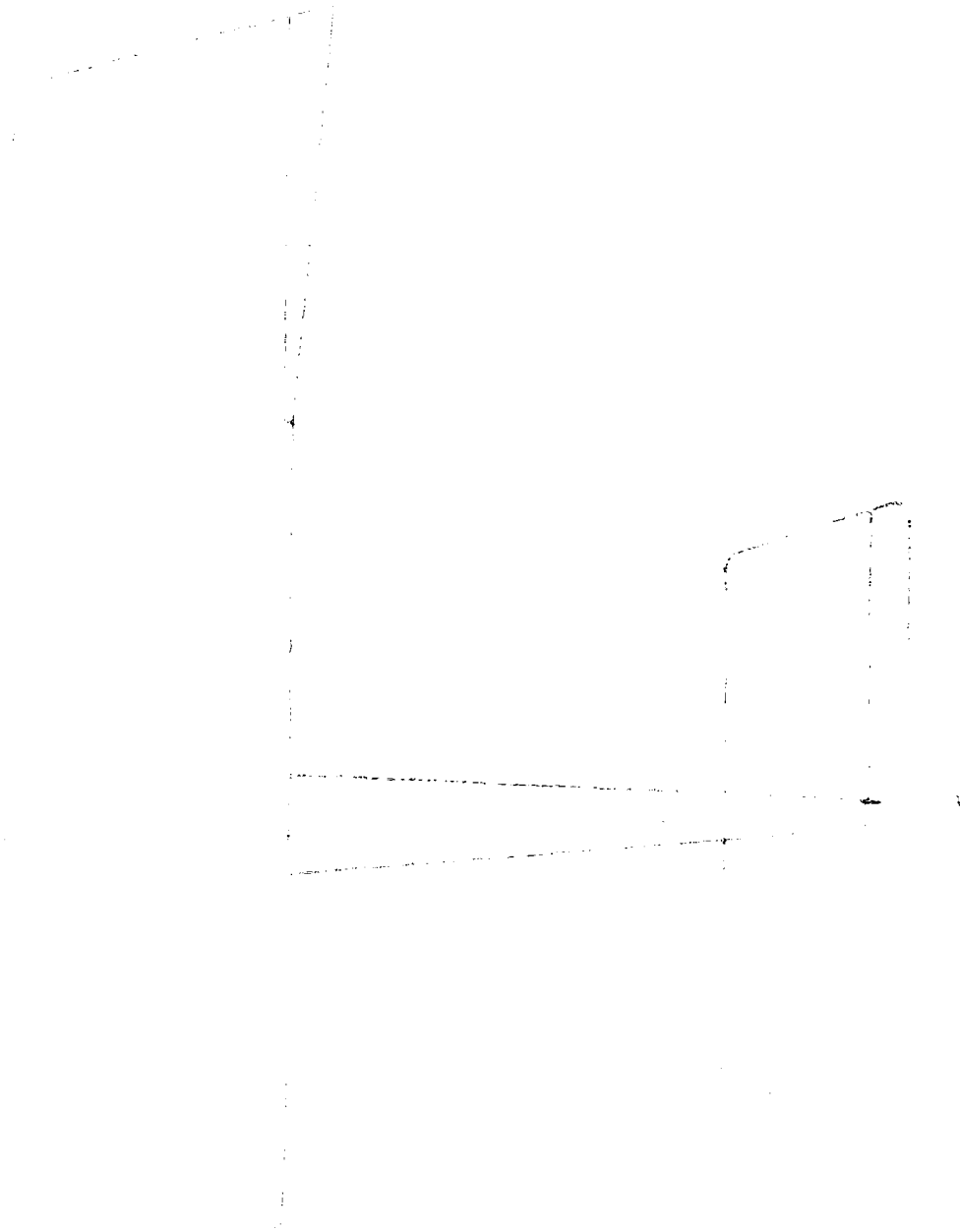
4. J. H. Davenport, "The Dynamics of Shipboard Control Systems," *Journal of Ship Research*, Vol. 1, No. 1, 1957, pp. 1-10.

5. J. H. Davenport, "The Dynamics of Shipboard Control Systems," *Journal of Ship Research*, Vol. 1, No. 1, 1957, pp. 1-10.

APPENDICES

10-1-10

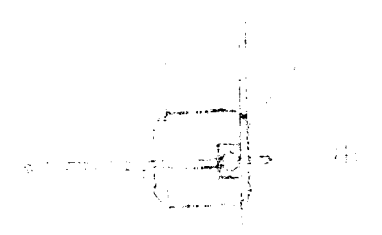
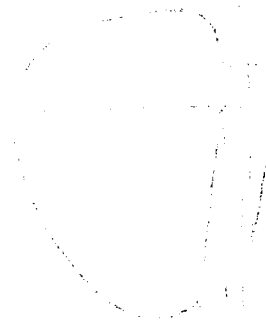
APPENDIX A - 100 SCALE AND 1000 SCALE DRAWINGS



1. 10/10/10

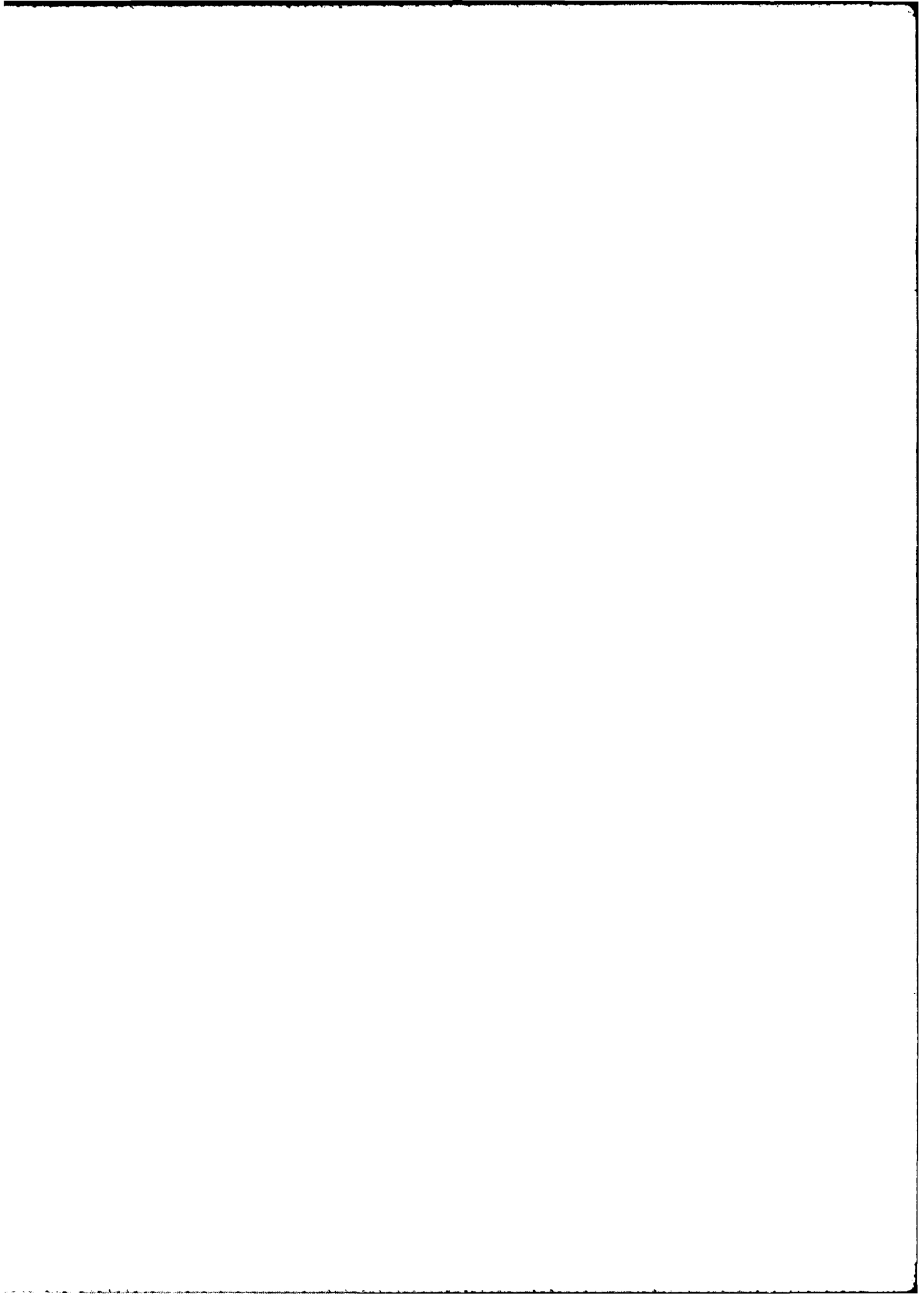
10/10/10

10/10/10



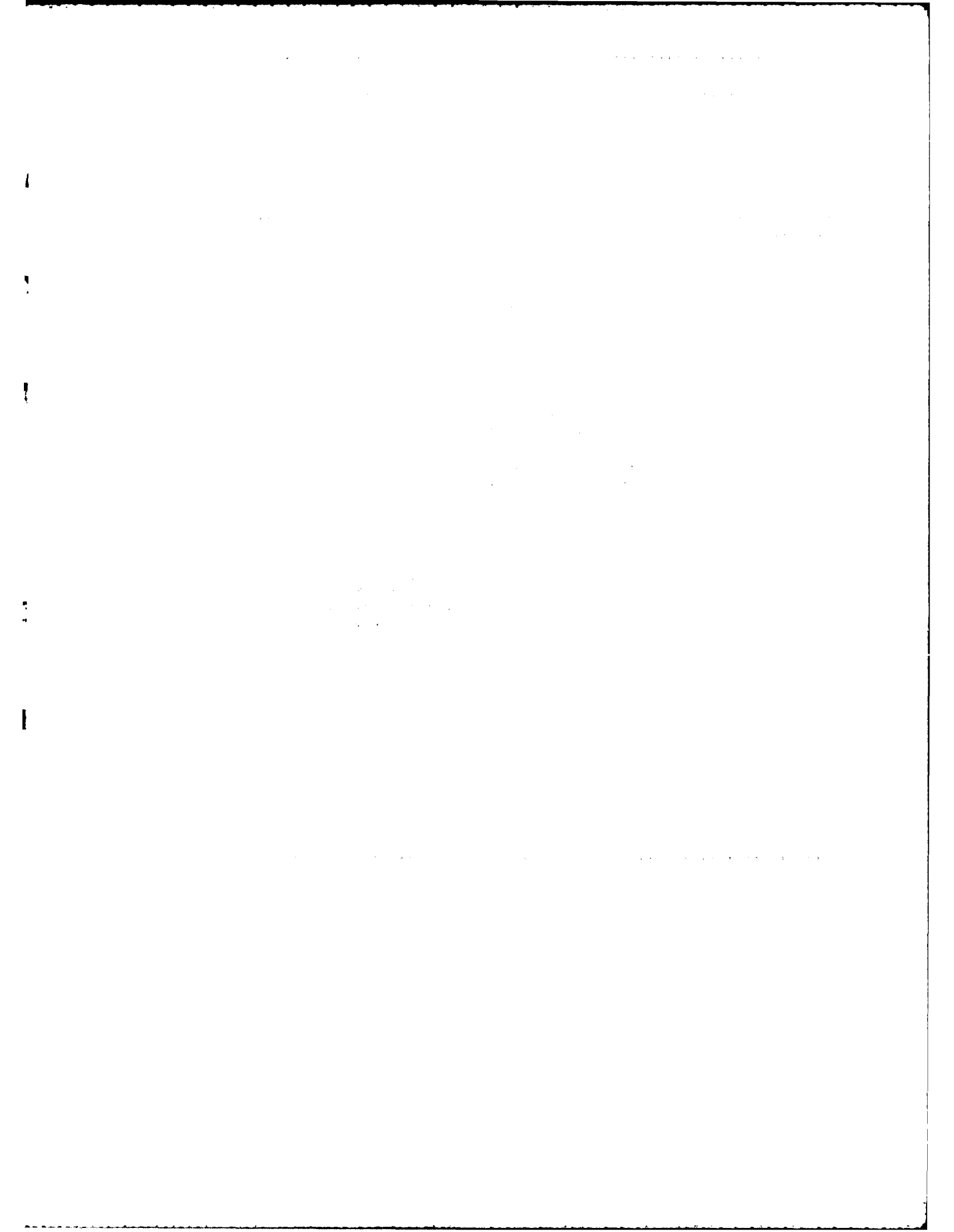
10/10/10











[illegible]

Figure 1. The effect of the number of trials on the number of correct responses. The number of correct responses was plotted against the number of trials for each condition. The number of correct responses increased with the number of trials for all conditions. The number of correct responses was highest for the condition with the highest number of trials (10 trials) and lowest for the condition with the lowest number of trials (2 trials).

===== File - DSNUMINT =====

```

100 #RESET FREE
200 FILE 4(TITLE="CONSTN.",KIND="DISK",FILETYPE=7)
300 FILE 5(TITLE="SYSDAT.",KIND="DISK",FILETYPE=7)
400 FILE 6(KIND="PRINTER")
500 FILE 7(KIND="REMOTE")
600 FILE 8(KIND="REMOTE")
700 #INCLUDE "PLOT/INCLUDE/FORTRAN."
800 #INCLUDE "(AERO457) DEAN/PLOTTER"
800 C *****
900 C ***FOLLOWING IS A LIST OF VARIABLE NAMES AND USES IN MAIN PROGRAM***
1000 C DT = STEP SIZE IN NUMERICAL INTEGRATION
1100 C T = TIME THE INTEGRATION IS CURRENTLY AT
1200 C X = STATE VAR. ARRAY- U,V,W,F,C,R,PSI,THE,PHI,N,E,H
1300 C DX = DERIVATIVES OF X
1400 C DE,BHP,DA,DR = AIRCRAFT CONTROLS
1500 C DETRM,BHPTRM,ETC. = TRIM SETTINGS FOR CONTROLS
1600 C AKROOT,AKV,ETC. = AUTO PILOT CONTROL GAINS
1700 C IX = VARIABLE OR CONTROL TO BE PLOTTED
1800 C AUTO,VELC,PSIC = COMMANDS TO FLY (ALT,VEL,HEADING)
1900 C TMAX = THE TIME LIMIT FOR THE INTEGRATION
2000 C ALTSPEC(S) = SELECTION FOR LR (1), HP (2), BOTH (3)
2100 C NSPP = NUMBER OF POINTS PLOTTED
2200 C NPTS = CURRENT POINT NUMBER COUNTER
2300 C NDIM = 12, THE DIMENSION OF X AND DX
2400 C ICNT = CURRENT LOOP NUMBER COUNTER
2500 C XP = ARRAY STORING THE DESIRED X POINTS
2600 C TP = ARRAY STORING THE DESIRED T POINTS
2700 C *****
2800 C *****
2900 DIMENSION X(12),DX(12),ERR(12),XP(1,250),TP(1,250),ALTSPEC(5)
3000 CHARACTER*60 TITLE(4),XTITLE(4),LABEL(4),LINE(4),LINE(4),TLIN(4)
3100 COMMON /BLK12/ DBN,ALON,CLOC,AVEL,ACLOC,CE,CM,CMA,CMA,CMD,
3200 1 CMCE,CYB,CYR,CYS,COR,CUR,CUR,CUR,CUR,CUR,CUR,CUR,CUR,
3300 2 CNR,CNR,CNR,CNR,CNR,CNR,CNR,CNR,CNR,CNR,CNR,CNR,
3400 3 CA,DE,DR,BHA
3500 DATA LABEL(1),XTITLE(1),TITLE(1),LINE(1),LINE(1),TLIN(1)
3600 DATA XTITLE(2),TITLE(2),TITLE(2),LINE(2),LINE(2),TLIN(2)
3700 DATA XTITLE(3),TITLE(3),TITLE(3),LINE(3),LINE(3),TLIN(3)
3800 C *****
3900 C *****
4000 C POINT IN THE DATA
4100 C *****
4200 C 1. 1. 1. 1. 1. 1. 1. 1. 1. 1. 1. 1.
4300 C 2. 2. 2. 2. 2. 2. 2. 2. 2. 2. 2. 2.
4400 C 3. 3. 3. 3. 3. 3. 3. 3. 3. 3. 3. 3.
4500 C 4. 4. 4. 4. 4. 4. 4. 4. 4. 4. 4. 4.
4600 C 5. 5. 5. 5. 5. 5. 5. 5. 5. 5. 5. 5.
4700 C 6. 6. 6. 6. 6. 6. 6. 6. 6. 6. 6. 6.
4800 C 7. 7. 7. 7. 7. 7. 7. 7. 7. 7. 7. 7.
4900 C 8. 8. 8. 8. 8. 8. 8. 8. 8. 8. 8. 8.
5000 C 9. 9. 9. 9. 9. 9. 9. 9. 9. 9. 9. 9.
5100 C 10. 10. 10. 10. 10. 10. 10. 10. 10. 10. 10. 10.
5200 C 11. 11. 11. 11. 11. 11. 11. 11. 11. 11. 11. 11.
5300 C 12. 12. 12. 12. 12. 12. 12. 12. 12. 12. 12. 12.
5400 C 13. 13. 13. 13. 13. 13. 13. 13. 13. 13. 13. 13.
5500 C 14. 14. 14. 14. 14. 14. 14. 14. 14. 14. 14. 14.
5600 C 15. 15. 15. 15. 15. 15. 15. 15. 15. 15. 15. 15.
5700 C 16. 16. 16. 16. 16. 16. 16. 16. 16. 16. 16. 16.
5800 C 17. 17. 17. 17. 17. 17. 17. 17. 17. 17. 17. 17.
5900 C 18. 18. 18. 18. 18. 18. 18. 18. 18. 18. 18. 18.
6000 C 19. 19. 19. 19. 19. 19. 19. 19. 19. 19. 19. 19.
6100 C 20. 20. 20. 20. 20. 20. 20. 20. 20. 20. 20. 20.
6200 C 21. 21. 21. 21. 21. 21. 21. 21. 21. 21. 21. 21.
6300 C 22. 22. 22. 22. 22. 22. 22. 22. 22. 22. 22. 22.
6400 C 23. 23. 23. 23. 23. 23. 23. 23. 23. 23. 23. 23.
6500 C 24. 24. 24. 24. 24. 24. 24. 24. 24. 24. 24. 24.
6600 C 25. 25. 25. 25. 25. 25. 25. 25. 25. 25. 25. 25.
6700 C 26. 26. 26. 26. 26. 26. 26. 26. 26. 26. 26. 26.
6800 C 27. 27. 27. 27. 27. 27. 27. 27. 27. 27. 27. 27.
6900 C 28. 28. 28. 28. 28. 28. 28. 28. 28. 28. 28. 28.
7000 C 29. 29. 29. 29. 29. 29. 29. 29. 29. 29. 29. 29.
7100 C 30. 30. 30. 30. 30. 30. 30. 30. 30. 30. 30. 30.
7200 C 31. 31. 31. 31. 31. 31. 31. 31. 31. 31. 31. 31.
7300 C 32. 32. 32. 32. 32. 32. 32. 32. 32. 32. 32. 32.
7400 C 33. 33. 33. 33. 33. 33. 33. 33. 33. 33. 33. 33.
7500 C 34. 34. 34. 34. 34. 34. 34. 34. 34. 34. 34. 34.
7600 C 35. 35. 35. 35. 35. 35. 35. 35. 35. 35. 35. 35.
7700 C 36. 36. 36. 36. 36. 36. 36. 36. 36. 36. 36. 36.
7800 C 37. 37. 37. 37. 37. 37. 37. 37. 37. 37. 37. 37.
7900 C 38. 38. 38. 38. 38. 38. 38. 38. 38. 38. 38. 38.
8000 C 39. 39. 39. 39. 39. 39. 39. 39. 39. 39. 39. 39.
8100 C 40. 40. 40. 40. 40. 40. 40. 40. 40. 40. 40. 40.
8200 C 41. 41. 41. 41. 41. 41. 41. 41. 41. 41. 41. 41.
8300 C 42. 42. 42. 42. 42. 42. 42. 42. 42. 42. 42. 42.
8400 C 43. 43. 43. 43. 43. 43. 43. 43. 43. 43. 43. 43.
8500 C 44. 44. 44. 44. 44. 44. 44. 44. 44. 44. 44. 44.
8600 C 45. 45. 45. 45. 45. 45. 45. 45. 45. 45. 45. 45.
8700 C 46. 46. 46. 46. 46. 46. 46. 46. 46. 46. 46. 46.
8800 C 47. 47. 47. 47. 47. 47. 47. 47. 47. 47. 47. 47.
8900 C 48. 48. 48. 48. 48. 48. 48. 48. 48. 48. 48. 48.
9000 C 49. 49. 49. 49. 49. 49. 49. 49. 49. 49. 49. 49.
9100 C 50. 50. 50. 50. 50. 50. 50. 50. 50. 50. 50. 50.
9200 C 51. 51. 51. 51. 51. 51. 51. 51. 51. 51. 51. 51.
9300 C 52. 52. 52. 52. 52. 52. 52. 52. 52. 52. 52. 52.
9400 C 53. 53. 53. 53. 53. 53. 53. 53. 53. 53. 53. 53.
9500 C 54. 54. 54. 54. 54. 54. 54. 54. 54. 54. 54. 54.
9600 C 55. 55. 55. 55. 55. 55. 55. 55. 55. 55. 55. 55.
9700 C 56. 56. 56. 56. 56. 56. 56. 56. 56. 56. 56. 56.
9800 C 57. 57. 57. 57. 57. 57. 57. 57. 57. 57. 57. 57.
9900 C 58. 58. 58. 58. 58. 58. 58. 58. 58. 58. 58. 58.

```

APPENDIX D- Simulation Program

This nonlinear simulation program was written in FORTRAN 77 for the Burroughs 6900 computer at the Air Force Academy by Cadet First Class Daniel A. Draeger. The program numerically integrates the six aircraft equations of motion for u , v , and w (velocity components in body axes) and for p , q , and r (rotational rates in body axes). Six kinematic equations are also integrated to get the Euler angles ϕ , θ , and ψ ; and displacements in the earth axes: altitude (h), north distance (N), and east distance (E). The results of simulation runs are delivered in graphical form using plotting routines not included in the listing. The aircraft data are read in from separate data files, a feature which allows the program to be used to simulate other aircraft. The twelve equations solved by the program are listed below in general form (Reference 1).

$m(\dot{u} - v r + w q) = \text{forces in x direction}$
 $m(\dot{v} + u r - w p) = \text{forces in y direction}$
 $m(\dot{w} - u q + v p) = \text{forces in z direction}$

$I_{xx}\dot{p} - I_{xz}\dot{r} - I_{xz}pq + (I_{zz} - I_{yy})rq = \text{moment about x axis}$

$I_{yy}\dot{q} + (I_{xx} - I_{zz})pr + I_{xz}(p^2 - r^2) = \text{moment about y axis}$

$I_{zz}\dot{r} - I_{xz}\dot{p} + (I_{yy} - I_{xx})pq + I_{xz}qr = \text{moment about z axis}$

$t = (t_0 \sin \delta + t_0 \cos \delta) \text{ sec}$
 $\phi = \phi_0 \cos \delta + \theta \sin \delta$
 $\psi = \psi_0 + \phi \sin \delta \tan \delta + \theta \cos \delta \tan \delta$

$h = h_0 + \int_0^t (u \sin \phi \cos \theta + v \sin \phi \sin \theta + w \cos \phi) dt$
 $N = N_0 + \int_0^t (u \cos \phi \cos \theta + v \cos \phi \sin \theta + w \sin \phi) dt$
 $E = E_0 + \int_0^t (-u \sin \phi \sin \theta + v \sin \phi \cos \theta + w \sin \phi) dt$

$$Y_B = \frac{\bar{q}_1 SC_{y_B}}{m} \text{ (ft sec}^{-2}\text{)}$$

$$Y_P = \frac{\bar{q}_1 SbC_{y_P}}{2mU_1} \text{ (ft sec}^{-1}\text{)}$$

$$Y_R = \frac{\bar{q}_1 SbC_{y_R}}{2mU_1} \text{ (ft sec}^{-1}\text{)}$$

$$Y_{\delta_a} = \frac{\bar{q}_1 SC_{y_{\delta_a}}}{m} \text{ (ft sec}^{-2}\text{deg}^{-1}\text{)}$$

$$Y_{\delta_r} = \frac{\bar{q}_1 SC_{y_{\delta_r}}}{m} \text{ (ft sec}^{-2}\text{deg}^{-1}\text{)}$$

$$L_B = \frac{\bar{q}_1 SbC_{l_B}}{I_{xx}} \text{ (sec}^{-2}\text{)}$$

$$L_P = \frac{\bar{q}_1 Sb^2 C_{l_P}}{2I_{xx}U_1} \text{ (sec}^{-1}\text{)}$$

$$L_R = \frac{\bar{q}_1 Sb^2 C_{l_R}}{2I_{xx}U_1} \text{ (sec}^{-1}\text{)}$$

$$L_{\delta_a} = \frac{\bar{q}_1 SbC_{l_{\delta_a}}}{I_{xx}} \text{ (sec}^{-2}\text{deg}^{-1}\text{)}$$

$$L_{\delta_r} = \frac{\bar{q}_1 SbC_{l_{\delta_r}}}{I_{xx}} \text{ (sec}^{-2}\text{deg}^{-1}\text{)}$$

$$N_B = \frac{\bar{q}_1 SbC_{n_B}}{I_{zz}} \text{ (sec}^{-2}\text{)}$$

$$N_{T_B} = \frac{\bar{q}_1 StC_{n_{T_B}}}{I_{zz}} \text{ (sec}^{-2}\text{)}$$

$$N_P = \frac{\bar{q}_1 Sb^2 C_{n_P}}{2I_{zz}U_1} \text{ (sec}^{-1}\text{)}$$

$$N_R = \frac{\bar{q}_1 Sb^2 C_{n_R}}{2I_{zz}U_1} \text{ (sec}^{-1}\text{)}$$

$$N_{\delta_a} = \frac{\bar{q}_1 SbC_{n_{\delta_a}}}{I_{zz}} \text{ (sec}^{-2}\text{deg}^{-1}\text{)}$$

$$N_{\delta_r} = \frac{\bar{q}_1 SbC_{n_{\delta_r}}}{I_{zz}} \text{ (sec}^{-2}\text{deg}^{-1}\text{)}$$

From Reference 1, the linearized lateral-directional equations of motion are (using the definitions from Table C-2):

$$U_1 \dot{\beta} + U_1 r = g \dot{\varphi} + Y_{\beta} \beta + Y_p p + Y_r r + Y_{\delta_a} \delta_a + Y_{\delta_r} \delta_r$$

$$\dot{p} - A_1 \dot{r} = L_{\beta} \beta + L_p p + L_r r + L_{\delta_a} \delta_a + L_{\delta_r} \delta_r$$

$$\dot{r} - B_1 \dot{p} = N_{\beta} \beta + N_T \beta + N_p p + N_r r + N_{\delta_a} \delta_a + N_{\delta_r} \delta_r$$

$$A_1 = \frac{I_{xz}}{I_{xx}}, \quad B_1 = \frac{I_{xz}}{I_{zz}}$$

In addition, the following approximations were added:

$$\begin{aligned} \dot{\varphi} &= p \\ \dot{\psi} &= r \end{aligned}$$

The values were substituted in and the equations were manipulated algebraically to obtain first order matrix form.

$$\begin{bmatrix} \dot{\beta} \\ \dot{p} \\ \dot{r} \\ \dot{\varphi} \\ \dot{\psi} \end{bmatrix} = \begin{bmatrix} -.5366 & -.000278 & -.9875 & .439 & 0 \\ -38.18 & -8.55 & 2.41 & 0 & 0 \\ 16.7 & .72 & -.448 & 0 & 0 \\ 0 & 1 & 0 & 0 & 0 \\ 0 & 0 & 1 & 0 & 0 \end{bmatrix} \begin{bmatrix} \beta \\ p \\ r \\ \varphi \\ \psi \end{bmatrix} + \begin{bmatrix} 0 & .00274 \\ 10.14 & .48 \\ -1.17 & -.157 \\ 0 & 0 \end{bmatrix} \begin{bmatrix} \delta_a \\ \delta_r \end{bmatrix}$$

Table C-1

$$x_u = \frac{-\bar{q}_1 S (C_{D_u} + 2C_{D_1})}{m U_1} (\text{sec}^{-1})$$

$$x_{T_u} = \frac{\bar{q}_1 S (C_{T_{x_u}} + 2C_{T_{x_1}})}{m U_1} (\text{sec}^{-1})$$

$$x_\alpha = \frac{-\bar{q}_1 S (C_{D_\alpha} - C_{L_1})}{m} (\text{ft sec}^{-2})$$

$$x_{\delta_e} = \frac{-\bar{q}_1 S C_{D_{\delta_e}}}{m} (\text{ft sec}^{-2} \text{deg}^{-1})$$

$$z_u = - \frac{\bar{q}_1 S (C_{L_u} + 2C_{L_1})}{m U_1} (\text{sec}^{-1})$$

$$z_\alpha = - \frac{\bar{q}_1 S (C_{L_\alpha} + C_{D_1})}{m} (\text{ft sec}^{-2})$$

$$z_{\dot{\alpha}} = - \frac{\bar{q}_1 S C_{L_{\dot{\alpha}}} \bar{c}}{2m U_1} (\text{ft sec}^{-1})$$

$$z_q = - \frac{\bar{q}_1 S C_{L_q} \bar{c}}{2m U_1} (\text{ft sec}^{-1})$$

$$z_{\delta_e} = - \frac{\bar{q}_1 S C_{L_{\delta_e}}}{m} (\text{ft sec}^{-2} \text{deg}^{-1})$$

$$M_u = \frac{\bar{q}_1 S \bar{c} (C_{m_u} + 2C_{m_1})}{I_{yy} U_1} (\text{ft}^{-1} \text{sec}^{-1})$$

$$M_{T_u} = \frac{\bar{q}_1 S \bar{c} (C_{m_{T_u}} + 2C_{m_{T_1}})}{I_{yy} I_1} (\text{ft}^{-1} \text{sec}^{-1})$$

$$M_\alpha = \frac{\bar{q}_1 S \bar{c} C_{m_\alpha}}{I_{yy}} (\text{sec}^{-2})$$

$$M_{T_\alpha} = \frac{\bar{q}_1 S \bar{c} C_{m_{T_\alpha}}}{I_{yy}} (\text{sec}^{-2})$$

$$\dot{M}_\alpha = \frac{\bar{q}_1 S \bar{c}^2 C_{m_\alpha}}{2I_{yy} U_1} (\text{sec}^{-1})$$

$$M_q = \frac{\bar{q}_1 S \bar{c}^2 C_{m_q}}{2I_{yy} U_1} (\text{sec}^{-1})$$

$$M_{\delta_e} = \frac{\bar{q}_1 S \bar{c} C_{m_{\delta_e}}}{I_{yy}} (\text{sec}^{-2} \text{deg}^{-1})$$

$$x_{T_{\delta_T}} = \frac{\bar{q}_1 S C_{T_{x_{\delta_T}}}}{m} (\text{ft sec}^{-2} \text{BHP}^{-1})$$

The remaining necessary coefficients and derivatives, listed below, were obtained by linearizing the drag polar around the steady-state condition and by assuming that the propeller thrust acts through the aircraft center of gravity.

$$\begin{aligned} C_{D_1} &= .073 & C_{m_1} &= 0 & C_{T_{x_1}} &= .073 \\ C_{D_\alpha} &= .259/\text{rad} & C_{m_{T_1}} &= 0 \\ C_{L_1} &= .376 & C_{m_{T_\alpha}} &= 0 \end{aligned}$$

From Reference 1, the linearized longitudinal equations of motion are (using the definitions from Table C-1):

$$\dot{U} = -g\theta + X_U U + X_{T_U} U + X_\alpha \alpha + X_{\delta_e} \delta_e + X_{T_{\delta_T}} \delta_T$$

$$U_1 \dot{\alpha} - U_1 q = Z_U U + Z_\alpha \alpha + Z_{\dot{\alpha}} \dot{\alpha} + Z_q q + Z_{\delta_e} \delta_e$$

$$\dot{q} = M_U U + M_{T_U} U + M_\alpha \alpha + M_{T_\alpha} \alpha + M_{\dot{\alpha}} \dot{\alpha} + M_q q + M_{\delta_e} \delta_e$$

In addition, the following approximations were added:

$$\dot{\theta} = q$$

$$\dot{h} = U_1 \theta - U_1 \alpha$$

The values were substituted in and the equations were manipulated algebraically to obtain first order matrix form.

$$\begin{bmatrix} \dot{q} \\ \dot{\theta} \\ \dot{U} \\ \dot{\alpha} \\ \dot{h} \end{bmatrix} = \begin{bmatrix} -3.733 & 0 & .01189 & -1.341 & 0 \\ 1 & 0 & 0 & 0 & 0 \\ 0 & -32.2 & -.2566 & 10.01 & 0 \\ .9193 & 0 & -.01169 & -4.642 & 0 \\ 0 & 73.33 & 0 & -73.33 & 0 \end{bmatrix} \begin{bmatrix} q \\ \theta \\ U \\ \alpha \\ h \end{bmatrix} + \begin{bmatrix} -.2033 & 0 \\ 0 & 0 \\ -.0257 & 5.63 \\ -.0057 & 0 \\ 0 & 0 \end{bmatrix} \begin{bmatrix} \delta_e \\ \delta_T \end{bmatrix}$$

3. Estimated Aerodynamic Data (Reference 1 and 5):

$$C_{m_u} = C_{L_u} = C_{D_u} = C_{m_{T_u}} = C_{m_{T_\alpha}} = 0$$

$$C_{m_{\dot{\alpha}}} = -4.0$$

$$C_{n_{T_\beta}} = 0$$

$$C_{m_q} = -11.0$$

$$C_{n_r} = -.046$$

$$C_{L_{\dot{\alpha}}} = 1.66$$

$$C_{n_p} = -.03$$

$$C_{L_q} = 4.16$$

$$C_{\ell_\beta} = -.078/\text{rad}^*$$

$$C_{T_{x_u}} = -.22$$

$$C_{\ell_p} = -.36$$

$$C_{y_p} = -.004$$

$$C_{\ell_r} = .096$$

$$C_{y_r} = .18$$

$$C_{T_{x_{\delta_T}}} = .066/\text{BHP}$$

*wind tunnel data not used because model had no wing dihedral

4. Mass Data (Reference 4):

$$\text{rolling moment of inertia } (I_{xx}) = 1.7 \text{ slg-ft}^2$$

$$\text{pitching moment of inertia } (I_{yy}) = 6.8 \text{ slg-ft}^2$$

$$\text{yawing moment of inertia } (I_{zz}) = 9.3 \text{ slg-ft}^2$$

$$\text{product of inertia } (I_{xz}) = 0$$

note: these inertia terms are relative to body axes

APPENDIX C- Aircraft Linearized Equations of Motion

The methods of Reference 1 were used to linearize the aircraft equations of motion about a steady-state condition of coordinated, straight and level flight at 7500 feet and 73.33 ft/s (50 mph). The angle of attack required for this condition was 7.2 degrees relative to body axes. Since the linearized model uses stability axes (longitudinal axis parallel to the steady-state relative wind), the inertia terms I_{xx} , I_{zz} , and I_{xz} , of Appendix B had to be transformed from body axes to stability axes.

-1.128241961 J 0
 -1.915390605 J -1.551649739
 -1.915390605 J 1.551649739
 -1.91013555 J 0
 -5.24272001 J 0

KHD = -.2 DEG / FT/SEC
 KH = .2 FT/SEC / FT
 KV = .1 BHP / FT/SEC

1 S**5 + 9.11187873 S**4 + 25.3997775 S**3 + 29.6077331 S**2 + 15.5221765 S + 1.95593185

POLES ARE:

-2.00669996 J 0
 -5.23439389 J 0
 -.846614841 J -1.57618756
 -.846614841 J 1.57618756
 -.177555202 J 0

KHD = -.2 DEG / FT/SEC
 KH = .25 FT/SEC / FT
 KV = .1 BHP / FT/SEC

1 S**5 + 9.11187873 S**4 + 25.3955989 S**3 + 29.6009527 S**2 + 16.2064611 S + 2.44491481

POLES ARE:

-2.08932918 J 0
 -5.22595506 J 0
 -.783362962 J -1.60383671
 -.783362962 J 1.60383671
 -.229868565 J 0

KHD = -.2 DEG / FT/SEC
 KH = .3 FT/SEC / FT
 KV = .1 BHP / FT/SEC

1 S**5 + 9.11187873 S**4 + 25.3914204 S**3 + 29.5941724 S**2 + 16.8907457 S + 2.93389777

POLES ARE:

-2.16250743 J 0
 -5.21739973 J 0
 -.724015404 J -1.625789061
 -.724015404 J 1.625789061
 -.280940771 J 0

KHD = -.2 DEG / FT/SEC
 KH = .2 FT/SEC / FT
 KV = .14 BHP / FT/SEC

1 S**5 + 8.77316074 S**4 + 22.5915516 S**3 + 23.3513994 S**2 + 10.872586 S + 1.02599105

POLES ARE:

-1.123213703 1 0
-1.720633944 1 -1.535506228
-1.720633944 1 .535506228
-1.97301432 1 0
-5.23566482 1 0

KHD = -.2 DEG / FT/SEC

KH = .2 FT/SEC / FT

KV = .06 BHP / FT/SEC

1 S**5 + 8.88606673 S**4 + 23.5276269 S**3 + 25.436844 S**2 + 12.4255646 S + 1.33596465

POLES ARE:

-1.145187511 1 0
-1.761329061 1 -1.553845598
-1.761329061 1 .553845598
-1.98295914 1 0
-5.23526197 1 0

KHD = -.2 DEG / FT/SEC

KH = .2 FT/SEC / FT

KV = .06 BHP / FT/SEC

1 S**5 + 8.99897273 S**4 + 24.4637022 S**3 + 27.5222885 S**2 + 13.9738705 S + 1.64594825

POLES ARE:

-1.9941163 1 0
-5.23483885 1 0
-1.803528034 1 -1.56736352
-1.803528034 1 .56736352
-1.162961521 1 0

KHD = -.2 DEG / FT/SEC

KH = .2 FT/SEC / FT

KV = .1 BHP / FT/SEC

1 S**5 + 9.11187677 S**4 + 25.3597775 S**3 + 29.6077331 S**2 + 15.5221765 S + 1.95593185

POLES ARE:

-2.00664997 1 0
-5.103429263 1 0
-1.846614619 1 -1.576187561
-1.846614619 1 .576187561
-1.177505202 1 0

KHD = -.2 DEG / FT/SEC

KH = .2 FT/SEC / FT

KV = .12 BHP / FT/SEC

1 S**5 + 9.01418473 S**4 + 26.3258527 S**3 + 31.5931176 S**2 + 14.0704824 S + 2.26591545

FOLES ARE:

-5.8008353 J -580455601
-5.89083331 J -580455601
-5.23392534 J 0
-2.12007073 J 0
-1.18704689 J 0

KR = 1.2 DEG / FT/SEC

KH = 1.2 FT/SEC / FT

KV = 1.14 BHP / FT/SEC

1.5**5 + 9.33769073 S**4 + 27.271928 S**3 + 33.7786222 S**2 + 16.6187683 S + 2.57589904

FOLES ARE:

-5.93523349 J -580293241
-5.933523349 J -580293241
-5.2334311 J 0
-2.33714597 J 0
-1.144966766 J 0

KR = 1.2 DEG / FT/SEC

KH = 1.2 FT/SEC / FT

KV = 1.15 BHP / FT/SEC

1.5**5 + 9.45059674 S**4 + 26.2080033 S**3 + 35.8640668 S**2 + 20.1670943 S + 2.68588265

FOLES ARE:

-5.23290956 J 0
-5.976525123 J -576609024
-5.976525123 J -576809024
-2.05591145 J 0
-1.20872506 J 0

Lateral-directional Poles

KNY = 0 DEG/s
KR = 0 DEG/RAD/s
KPSI = 0 RAD/s/RAD
KYD = 0 DEG/RAD/s
1 S**5 + 9.5346 S**4 + 23.4041628 S**3 + 131.745946 S**2 + -10.159496 S + 0

POLES ARE:
.0760546455 j 0
-1.500580503 j -3.90704845
-1.500580503 j 3.90704845
-8.60949365 j 0
0 j 0

KNY = 0 DEG/s
KR = 1 DEG/RAD/s
KPSI = 1 RAD/s/RAD
KYD = -20 DEG/RAD/s
1 S**5 + 11.5046 S**4 + 40.6514048 S**3 + 134.318141 S**2 + 26.6701227 S + 5.47289886

POLES ARE:
-8.54374773 j 0
-1.38137235 j -3.58688741
-1.38137235 j 3.58688741
-0.990537396 j -1.183157467
-0.990537396 j 1.183157467

KNY = 1 DEG/s
KR = 1 DEG/RAD/s
KPSI = 1 RAD/s/RAD
KYD = 1 DEG/RAD/s
1 S**5 + 11.627947 S**4 + 44.659137 S**3 + 150.239301 S**2 + 30.1706697 S + 8.06247998

POLES ARE:
-0.990537396 j 0
-1.38137235 j -3.58688741
-1.38137235 j 3.58688741
-0.990537396 j -1.183157467
-0.990537396 j 1.183157467

KNY = 2 DEG/s
KR = 2 DEG/RAD/s
KPSI = 2 RAD/s/RAD
KYD = 2 DEG/RAD/s
1 S**5 + 12.1075451 S**4 + 47.2770816 S**3 + 168.404667 S**2 + 34.1706547 S + 8.71616742

POLES ARE:

-8.64578947 j 0
-1.64450809 j -3.95216212
-1.64450809 j 3.95216212
-.101569701 j -.179452201
-.101569701 j .179452201

KNY = 30 DEG/s

KR = 1 DEG/RAD/S

KPSI = .1 RAD/S /RAD

KYD = 20 DEG/RAD/S

1 S**5 + 11.5075614 S**4 + 54.4966084 S**3 + 189.418558 S**2 + 38.7851716 S + 7.51334065

POLES ARE:

-8.21027749 j 0
-1.80600033 j -4.14745607
-1.80600033 j 4.14745607
-.10266164 j -.177803379
-.10266164 j .177803379

KNY = 40 DEG/s

KR = 1 DEG/RAD/S

KPSI = .1 RAD/S /RAD

KYD = 20 DEG/RAD/S

1 S**5 + 11.9610645 S**4 + 60.8427901 S**3 + 213.897442 S**2 + 44.1676258 S + 8.41982831

POLES ARE:

-8.06719367 j 0
-1.94370007 j -4.18188056
-1.94370007 j 4.18188056
-.10166163 j -.176871479
-.10166163 j .176871479

KNY = 50 DEG/s

KR = 1 DEG/RAD/S

KPSI = .1 RAD/S /RAD

KYD = 20 DEG/RAD/S

1 S**5 + 13.5188797 S**4 + 67.9042413 S**3 + 242.818953 S**2 + 50.5271121 S + 9.49083428

POLES ARE:

-8.68828769 j 0
-2.11444504 j -4.50544296
-2.11444504 j 4.50544296
-.104781131 j -.174847122
-.104781131 j .174847122

KNY = 60 DEG/s

KR = 1 DEG/RAD/S

KPI = 1.1 RAD S RAD
 KPI = 1.1 RAD S RAD S
 1.5**5 + 14.1515127 S**4 + 76.5145123 S**3 + 277.513.18 S**2 + 58.156.149 S + 10.775616

POLLS ARE:
 -8.9915778 j 0
 -2.4712136y j -4.76718744
 -3.47226309 j 4.76718744
 -1.05429385 j -1.173509154
 -1.05429385 j 1.173509154

KPI = 1.0 DEB RAD S
 KPI = 1.1 RAD S RAD
 KPI = 1.1 DEB RAD S
 1.5**5 + 11.9955614 S**4 + 55.9236229 S**3 + 190.287321 S**2 + 8.89488741 S + 4.50600439

POLLS ARE:
 -1.44121 j 0
 -1.95144 j 4.11124402
 -1.95144 j 4.11124402
 -1.919951268 j -1.153661036
 -1.919951268 j 1.153661036

KPI = 1.0 DEB
 KPI = 1.0 DEB RAD S
 KPI = 1.1 RAD S RAD
 KPI = 1.0 DEB RAD S
 1.5**5 + 12.7515614 S**4 + 55.0102156 S**3 + 189.85297 S**2 + 23.7950296 S + 6.01067252

POLLS ARE:
 -3.92673673 j 0
 -1.89720673 j -4.17997346
 -1.89720673 j 4.17997346
 -1.09255227 j -1.170952076
 -1.09255227 j 1.170952076

KPI = 1.0 DEB
 KPI = 1.0 DEB RAD S
 KPI = 1.1 RAD S RAD
 KPI = 1.0 DEB RAD S
 1.5**5 + 12.7515614 S**4 + 55.0102156 S**3 + 189.85297 S**2 + 23.7950296 S + 6.01067252

POLLS ARE:
 -3.92673673 j 0
 -1.89720673 j -4.17997346
 -1.89720673 j 4.17997346
 -1.09255227 j -1.170952076
 -1.09255227 j 1.170952076

1. The first part of the document is a list of the names of the persons who were present at the meeting. The names are listed in alphabetical order.

2. The second part of the document is a list of the topics that were discussed at the meeting. The topics are listed in alphabetical order.

3. The third part of the document is a list of the actions that were taken at the meeting. The actions are listed in alphabetical order.

4. The fourth part of the document is a list of the dates when the actions were completed. The dates are listed in alphabetical order.

5. The fifth part of the document is a list of the names of the persons who were responsible for the actions. The names are listed in alphabetical order.

6. The sixth part of the document is a list of the names of the persons who were present at the meeting. The names are listed in alphabetical order.

7. The seventh part of the document is a list of the topics that were discussed at the meeting. The topics are listed in alphabetical order.

8. The eighth part of the document is a list of the actions that were taken at the meeting. The actions are listed in alphabetical order.

76

77

78

79

80

END

FILMED

7-35

DTIC